AD-755 117

THERMAL MONITORING OF GEOLOGICAL CHANGES DURING EXCAVATION

H. K. Lintz

Bendix Research Laboratories

Prepared for:

Advanced Research Projects Agency

October 1972

DISTRIBUTED BY:

NTIS

National Technical Information Service
U. S. DEPARTMENT OF COMMERCE
5285 Port Royal Road, Springfield Va. 22151

AD755117

Report No. 6318
Copy No.

BRL Project 2410

THERMAL MONITORING OF GEOLOGICAL CHANGES DURING EXCAVATION

Final Report

October 1972

Contract No. H0210031
Effective April 30, 1971
Terminates July 31 1972
Amount: $80,87[illegible]

Principal Investigator:

H. K. Lintz (313) 352-7764
Bendix Research Laboratories
Southfield, Michigan 48076

Project Engineer:
Robert H. Merrill

DDC
RECEIVED
FEB 13 1973
D

Sponsored by:
Advanced Research Projects Agency
ARPA Order No. 1579, Amend. 2
Program Code 1F10

Reproduced by
NATIONAL TECHNICAL
INFORMATION SERVICE
U S Department of Commerce
Springfield VA 22151

The views and conclusions contained in this document are those of the authors and should not be interpreted as necessarily representing the official policies either expressed or implied, of the Advanced Research Projects Agency or the U.S. Government.

DISTRIBUTION STATEMENT A
Approved for public release;
Distribution Unlimited

Unclassified

Security Classification

DOCUMENT CONTROL DATA - R&D

(Security classification of title, body of abstract and indexing annotation must be entered when the overall report is classified)

1. ORIGINATING ACTIVITY (Corporate author)

Bendix Research Laboratories
Southfield, Michigan 48076

2a. REPORT SECURITY CLASSIFICATION

Unclassified

2b. GROUP

3. REPORT TITLE

Thermal Monitoring of Geological Changes During Excavation

4. DESCRIPTIVE NOTES (Type of report and inclusive dates)

Final Report 30 April 1971 - 31 July 1972

5. AUTHOR(S) (Last name, first name, initial)

Lintz, H. K.

6. REPORT DATE	7a. TOTAL NO. OF PAGES	7b. NO. OF REFS
October 1972	65	7

8a. CONTRACT OR GRANT NO.	9a. ORIGINATOR'S REPORT NUMBER(S)
H0210031	
b. PROJECT NO. ARPA Order No. 1579, Amend. 2	6318
c. Program Code 1F10	9b. OTHER REPORT NO(S) (Any other numbers that may be assigned this report)
d.	

10. AVAILABILITY/LIMITATION NOTICES

Distribution of this report is unlimited.

11. SUPPLEMENTARY NOTES	12. SPONSORING MILITARY ACTIVITY
BRL Project 2410	Advanced Research Projects Agency Washington, D. C.

13. ABSTRACT

Monitoring or rock temperatures with a radiometer was investigated for its feasibility as a hazard prediction method during rapid excavation in hard rock.

It was found both theoretically and experimentally that errors introduced into the rock temperature measurements by heat exchange with the tunnel air, heat dissipation of machinery, heat generated by the excavation process itself, and moisture on the rock mask a wide range of temperature signals from actual hazardous changes in lithology.

The temperature monitoring method is not reliable enough for hazard prediction. However, indications are that it could be used to map out large volumes of different lithology, such as ore bodies, in mines.

Details of illustrations in this document may be better studied on microfiche.

DD FORM 1 JAN 64 1473

I-a

Unclassified

Security Classification

14. KEY WORDS	LINK A		LINK B		LINK C	
	ROLE	WT	ROLE	WT	ROLE	WT
Infrared Radiometer Rock Temperature Lode Detection Rapid Excavation Geothermal Sources Spalled Rock Ore Bodies Effect of Blasting on Rock Temperature						

INSTRUCTIONS

1. **ORIGINATING ACTIVITY:** Enter the name and address of the contractor, subcontractor, grantee, Department of Defense activity or other organization *(corporate author)* issuing the report.

2a. **REPORT SECURITY CLASSIFICATION:** Enter the overall security classification of the report. Indicate whether "Restricted Data" is included. Marking is to be in accordance with appropriate security regulations.

2b. **GROUP:** Automatic downgrading is specified in DoD Directive 5200.10 and Armed Forces Industrial Manual. Enter the group number. Also, when applicable, show that optional markings have been used for Group 3 and Group 4 as authorized.

3. **REPORT TITLE:** Enter the complete report title in all capital letters. Titles in all cases should be unclassified. If a meaningful title cannot be selected without classification, show title classification in all capitals in parenthesis immediately following the title.

4. **DESCRIPTIVE NOTES:** If appropriate, enter the type of report, e.g., interim, progress, summary, annual, or final. Give the inclusive dates when a specific reporting period is covered.

5. **AUTHOR(S):** Enter the name(s) of author(s) as shown on or in the report. Enter last name, first name, middle initial. If military, show rank and branch of service. The name of the principal author is an absolute minimum requirement.

6. **REPORT DATE:** Enter the date of the report as day, month, year; or month, year. If more than one date appears on the report, use date of publication.

7a. **TOTAL NUMBER OF PAGES:** The total page count should follow normal pagination procedures, i.e., enter the number of pages containing information.

7b. **NUMBER OF REFERENCES:** Enter the total number of references cited in the report.

8a. **CONTRACT OR GRANT NUMBER:** If appropriate, enter the applicable number of the contract or grant under which the report was written.

8b, 8c, & 8d. **PROJECT NUMBER:** Enter the appropriate military department identification, such as project number, subproject number, system numbers, task number, etc.

9a. **ORIGINATOR'S REPORT NUMBER(S):** Enter the official report number by which the document will be identified and controlled by the originating activity. This number must be unique to this report.

9b. **OTHER REPORT NUMBER(S):** If the report has been assigned any other report numbers *(either by the originator or by the sponsor)*, also enter this number(s).

10. **AVAILABILITY/LIMITATION NOTICES:** Enter any limitations on further dissemination of the report, other than those imposed by security classification, using standard statements such as:

(1) "Qualified requesters may obtain copies of this report from DDC."

(2) "Foreign announcement and dissemination of this report by DDC is not authorized."

(3) "U. S. Government agencies may obtain copies of this report directly from DDC. Other qualified DDC users shall request through _____."

(4) "U. S. military agencies may obtain copies of this report directly from DDC. Other qualified users shall request through _____."

(5) "All distribution of this report is controlled. Qualified DDC users shall request through _____."

If the report has been furnished to the Office of Technical Services, Department of Commerce, for sale to the public, indicate this fact and enter the price, if known.

11. **SUPPLEMENTARY NOTES:** Use for additional explanatory notes.

12. **SPONSORING MILITARY ACTIVITY:** Enter the name of the departmental project office or laboratory sponsoring *(paying for)* the research and development. Include address.

13. **ABSTRACT:** Enter an abstract giving a brief and factual summary of the document indicative of the report, even though it may also appear elsewhere in the body of the technical report. If additional space is required, a continuation sheet shall be attached.

It is highly desirable that the abstract of classified reports be unclassified. Each paragraph of the abstract shall end with an indication of the military security classification of the information in the paragraph, represented as *(TS)*, *(S)*, *(C)*, or *(U)*.

There is no limitation on the length of the abstract. However, the suggested length is from 150 to 225 words.

14. **KEY WORDS:** Key words are technically meaningful terms or short phrases that characterize a report and may be used as index entries for cataloging the report. Key words must be selected so that no security classification is required. Identifiers, such as equipment model designation, trade name, military project code name, geographic location, may be used as key words but will be followed by an indication of technical context. The assignment of links, rules, and weights is optional.

THERMAL MONITORING OF GEOLOGICAL CHANGES DURING EXCAVATION

Final Report

October 1972

Contract No. H0210031
Effective April 30, 1971
Terminates July 31, 1972
Amount: $80,875

Principal Investigator:

H. K. Lintz (313) 352-7764
Bendix Research Laboratories
Southfield, Michigan 48076

Project Engineer:
Robert H. Merrill

Sponsored by:
Advanced Research Projects Agency
ARPA Order No. 1579, Amend. 2
Program Code 1F10

The views and conclusions contained in this document are those of the authors and should not be interpreted as necessarily representing the official policies either expressed or implied, of the Advanced Research Projects Agency or the U.S. Government.

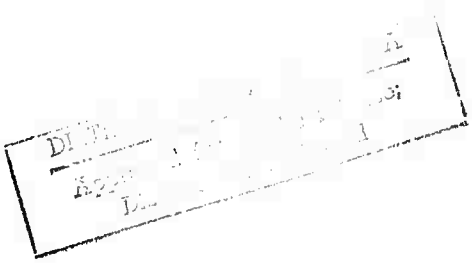

I-C

TABLE OF CONTENTS

	Page
SECTION 1 - TECHNICAL REPORT SUMMARY	1-1
SECTION 2 - THEORETICAL CONSIDERATIONS	2-1
2.1 General	2-1
2.2 Literature Survey	2-1
2.3 Theoretical Analysis of Lithologies with Different Thermal Conductivity	2-3
2.3.1 Model Containing a Spherical Intrusion	2-4
2.3.1.1 Location of Maximum Temperature Change	2-5
2.3.1.2 Temperature Variation as Function of Wall Thickness Between Tunnel and Inclusion (Tunnel Floor on Centerline)	2-8
2.3.1.3 Temperature Determination for the Case in which the Tunnel and the Inclusion have Equal Dimensions	2-10
2.3.1.4 Analytical Determination of the Location of the Obstacle	2-12
2.3.1.5 Determination of Error in Location Due to Temperature Error	2-16
2.3.2 Model Containing an Area of Cylindrical Shape	2-17
2.3.3 Temperature Variation as a Function of Wall Thickness Between Tunnel and Inclusion	2-18
2.3.4 Summary of Mathematical Analysis	2-20
2.4 A Uranium Ore Body as a Model of a Geothermal Source	2-20
SECTION 3 - INSTRUMENTATION SELECTION	3-1
3.1 Temperature Measuring Instrument and Procedure	3-1
3.2 Radiometer Corrections	3-2
SECTION 4 - EXPERIMENTAL FIELD TEST AND RESULTS	4-1
4.1 Sites of Measurements	4-1
4.1.1 Temperature Measurements on a Rock Surface with an Intrusion as well as Heavily Jointed and Solid Regions (Colorado School of Mines Experimental Mine)	4-4
4.1.2 Temperature Difference Between Loose Rock and Solid Rock	4-10

		Page
4.2	Temperature Mapping of an Unventilated Drift	4-13
4.3	Determination of Influence of Blasting on Rock Temperature Measurements	4-14
4.4	Temperature Mapping Across Large Intrusion at End of Drift B1	4-17
4.5	Temperature Mapping of a Bored Sloped Tube Penetrating a Magnetic Ore Body	4-17
4.6	Summary of Experimental Results	4-21
SECTION 5 - CONCLUSIONS		5-1
SECTION 6 - REFERENCES		6-1

LIST OF ILLUSTRATIONS

Figure No.	Title	Page
2-1	Heat Flow in a Homogeneous Medium	2-2
2-2	Distortion of Isotherms Around Area of Different κ	2-2
2-3	Distortion of Isotherms in Tunnel Approaching Area of Different κ	2-2
2-4	Geometrical Layout of Tunnel, Obstacle, and Temperature Measuring Points	2-6
2-5	Location of Points of Optimum Temperature Change	2-8
3-1	Experimental Setup in the Mine	3-4
4-1	Schematic of the Experimental Mine of the Colorado School of Mines	4-2
4-2	Schematic of Lithology Around Bored Tube	4-4
4-3	Feldspar Intrusion in Gneiss Matrix	4-5
4-4	First Sweep Over Feldspar Intrusion	4-7
4-5	Second Scan Over Feldspar Intrusion	4-9
4-6	Influence of Body Radiation on Rock Temperature Measurements	4-9
4-7	Sweep Over Feldspar Intrusion (No Personnel Present)	4-11
4-8	Schematic of Loose Rock	4-11
4-9	Apparent Temperature Distribution Along Drift 3A	4-15
4-10	Apparent Temperature Distribution Along Drift B1	4-15
4-11	Rock Appearance Prior to Blasting	4-16
4-12	Rock Exposed by Blasting	4-16
4-13	Diagram of Closed End of Drift B1	4-18
4-14	Bored Tube at Republic Steel Mine	4-18
4-15	Plot of Air Temperature and Rock Temperature for Bored Tube	4-19

Table No.	Title	Page
2-1	Temperature Values for Spherical Model	2-9
2-2	Calculations of Unknowns	2-15
2-3	Effect of Temperature Measurement Error on Calculated Coordinates	2-17
2-4	Temperature Values for Cylindrical Model	2-19
2-5	Properties of Uranium Isotopes	2-21
2-6	Uranium Decay Processes	2-22
3-1	Temperature Error as a Function of Emissivity	3-5

SECTION 1
TECHNICAL REPORT SUMMARY

The goal of this work was to predict hazardous changes in lithology ahead of tunnels in hard rock during rapid excavation. Based on the fact that any change in lithology also means a change of thermal properties in the affected regions, it follows that the temperature distribution in such rock formations is influenced in a characteristic way. The undisturbed temperature field in homogeneous isotropic rock would show isothermal planes parallel to the surface of the earth. Any inclusion in this otherwise homogeneous rock matrix will lead to curvature of the isotherms in the vicinity of the inclusion. Thus it was concluded that changes of lithology ahead of the excavation would show up as changes in the rock temperature of the tunnel walls. The kind of lithology changes to be predicted in hard rock were intrusions, fault zones, water courses, and gas seepage. From the study of investigations of temperature fields around differently shaped intrusions, it was concluded that all of the geological changes mentioned above fall into two categories:

- Regions in which only the thermal conductivity changes
- Regions with either heat sources or heat sinks.

The first category includes intrusions, fault zones, ore bodies, and water courses with no flow. Water courses with either flowing hot or cold water, and other geothermal sources form the second category.

Since the temperatures of geothermal sources can cover a very wide range of temperatures, one can only try to predict the presence of such sources by establishing boundaries up to which temperature changes can be caused by nongeothermal inclusions and assume that any temperature change exceeding these boundaries (a few hundredths of a °C) is caused by geothermal action. Therefore the analysis of an inclusion with different thermal conductivities seemed to be the most significant model to study the changes of temperature in the matrix rock. From this

this analysis, we arrived at the conclusion that the temperature measuring device, which was to be a radiometer, had to be able to measure temperature changes on the order of about 5×10^{-3}°C in order to predic. significant hazards. This value is very close to the highest sensitivity achievable with available radiometers. However, this was not considered an insurmountable obstacle considering that future development should result in instruments with higher sensitivity. A much more severe problem was expected from the influence of the tunnel environment, for example, ventilation, heat dissipation from the excavating process itself, and the unknown radiation properties of the rock materials in the infrared.

A number of temperature measurements were taken in the experimental mine of the Colorado School of Mines in order to determine the effect of the tunnel environment on rock temperature. Significant observations were made:

- Blasting changes the rock temperature in the vicinity of the shot holes considerably and obscures the true rock temperature for many hours.
- Changes in air temperatures caused by ventilation in drifts have long lasting effects on the rock temperature.
- The infrared radiation from people can result in apparent temperature signals many times the size of those caused by rock temperature changes.

The emissivity change due to slight changes in the composition of rock of the same lithology did not seem to influence temperature readings.

The measurements in the bored tube in the Republic Steel Mine in Mineville N.Y. showed that in the case of very large regions of lithology change, such as the huge ore body in the Republic Steel Mine, sufficient temperature change is created so that the presence of the ore body can be sensed behind other types of rock, provided there is no forced air flow in the tunnel.

The measurements in the Republic Steel Mine also showed that, if spalling occurs, the discovery of loose rock may not be possible. This

is due to the fact that large areas of drift walls can be covered by very thin sheets of spalled-off rock material which very quickly reach equilibrium temperature by heat exchange with air. These sheets therefore show the same temperature despite the fact that loose rock might lie underneath.

From the mathematical study and the on-site measurements, we have reached the conclusion that thermal monitoring as a method to predict hazards during excavation in hard rock is not reliable. The monitoring of rock temperatures in drifts seems to have potential for the securing of large ore bodies where the available time for measurements is long, and where the air flow can be controlled. However, the radiometer measurements may not be able to compete with gravitational or magnetic methods.

SECTION 2

THEORETICAL CONSIDERATIONS

2.1 GENERAL

The use of rock temperature measurements to predict regions of geological change in hard rock is based on the fact that a constant heat flow exists from the center of the earth to the surface. In a matrix rock, where the thermal conductivity is undisturbed, a parallel vertical heat flow with horizontal isotherms will exist (See Figure 2-1). If in this matrix a region exists which has a different lithology and thus a different thermal conductivity, then the isotherms are distorted as shown in Figure 2-2.

If a tunnel is excavated horizontally in an undisturbed matrix, then disregarding all possible disturbances, the temperature measured on a horizontal line along the tunnel is constant. If, however, a region of different lithology is present (Figure 2-3), then the isotherms are bent up and the temperature measured along the horizontal line increases. This increase in temperature is the signal used to predict the region of geological change.

In the following subsections, two models of regions with a geological change are analyzed in order to determine the kind of signal to be expected and how this signal can be evaluated to determine the size and location of the region. The numerical values used in the analysis are based on data obtained from a literature search.

2.2 LITERATURE SURVEY

A thorough study of tables and papers was performed to obtain both values of thermal conductivities of pure minerals as well as rocks consisting of more or less homogeneous mixtures of such minerals. Two important facts seem to emerge from this search, namely that in materials with the same mineralogical names, there was always a certain spread in

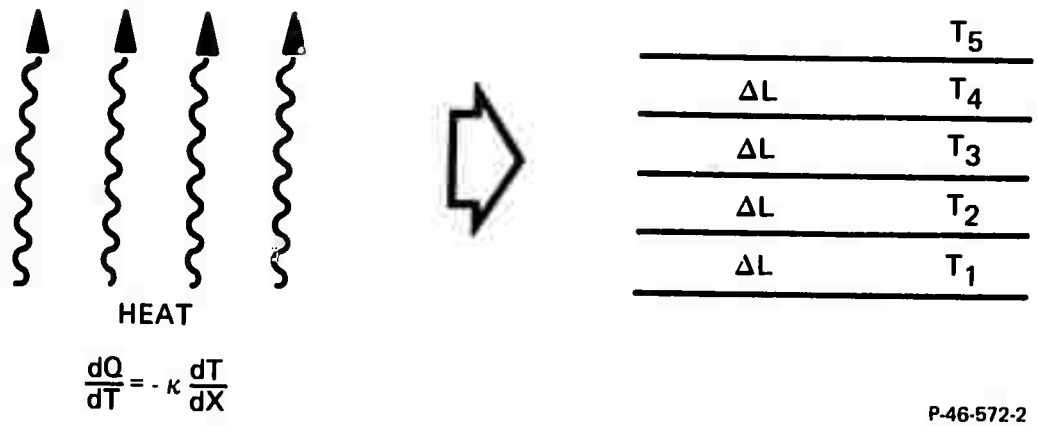

Figure 2-1 - Heat Flow in a Homogeneous Medium

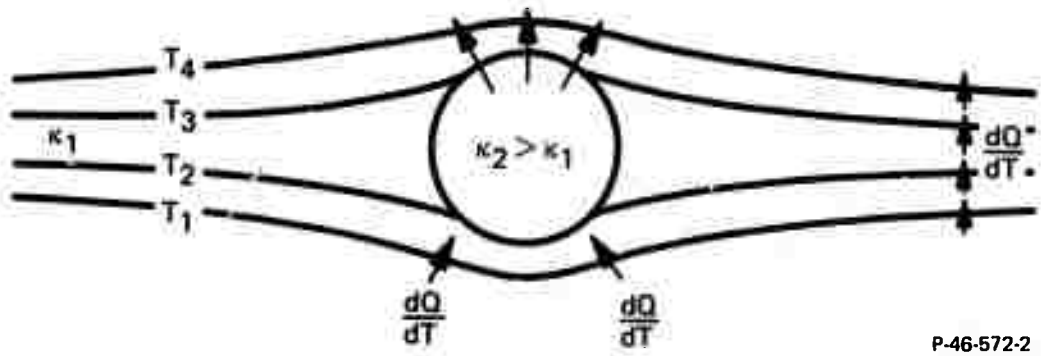

Figure 2-2 - Distortion of Isotherms Around Area of Different κ

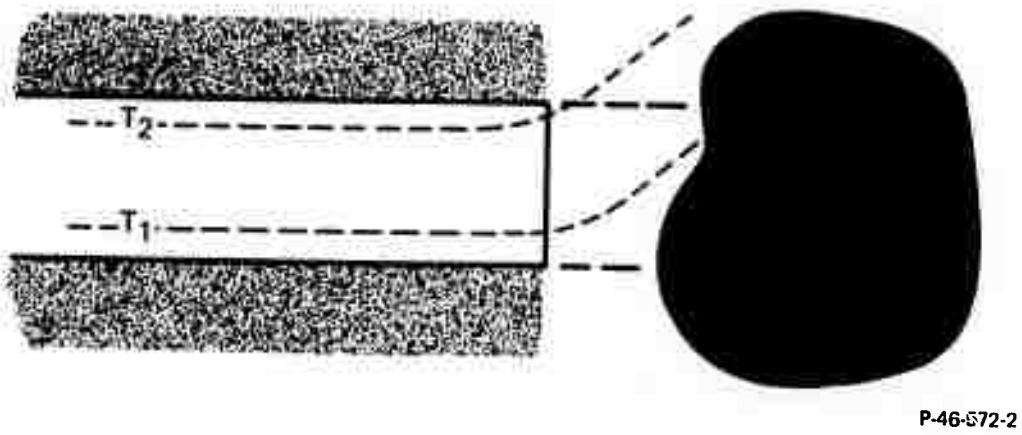

Figure 2-3 - Distortion of Isotherms in Tunnel Approaching Area of Different κ

values depending on the location from which they came and also to a somewhat lesser degree on the investigator. Even in areas where there was only one type of rock formation, the measured thermal conductivities of samples vary sometimes by as much as a factor of 1.5. It seems, however, that for hard rocks, the thermal conductivity ranges from 5 to 16 x 10^{-3} cal/cm sec °C.

Another area of interest is the magnitude of thermal gradients to be encountered in underground tunnels. Over the USA, one finds the range of thermal gradients:

Minimum:	New Mexico	- 8.0 x 10^{-3} °C/m
Maximum:	Eureka, Utah	- 80.0 x 10^{-3} °C/m
USA Average:		- 20 x 10^{-3} °C/m

The highest thermal gradients seem to occur in areas where many geothermal sources are known to exist. If these thermal gradients do not change rapidly from location to location within the tunnel, then the high values can be useful for the detection of geological changes.

Another area of literature search, namely the search for information on the effects of the tunnel environment on the detectable thermal gradient of the tunnel walls, yielded very few results. It is to be expected that the tunnel ventilation combined with possible humidity and the existence of a fractured layer on the tunnel walls will lead to local cooling or even heating, which, if occurring in an uncontrolled manner, are a perturbation on the tunnel wall temperature measurements. The size of these regions - if they exist - and their temperature deviation from the undisturbed case must be known, especially their magnitude, since they can obscure the sought-after temperature.

2.3 THEORETICAL ANALYSIS OF LITHOLOGIES WITH DIFFERENT THERMAL CONDUCTIVITY

In the theoretical analysis of temperature distributions in a hard rock matrix containing zones of lithologic change, one must assume some kind of idealized geometry. So long as the volume of different

geology is not a geothermal heat source or a fracture zone with substantial water flow or a large aquifer permitting convection, the different types of disturbances can be treated mathematically in the same fashion.

Since an infinite number of geometrically irregular configurations of inclusions can occur, this analysis is restricted to two basic models: the sphere and the cylinder.

Another important requirement is that the isotherms underground are not disturbed by the surface relief. Although corrections for certain types of surface reliefs are known[1], they are almost impossible to determine for practical cases in which the temperature has to be determined inside mountains but not far from the surface. Not only would one have to know the topography of the mountain quite accurately but would also have to consider the thermal characteristics of all the materials covering the surface. Also the geological history of the intrusion with respect to its age and initial temperature is not taken into account.[1]

In our models, we will assume a sufficient enough depth such that the surface structure will not have an effect on the shape of the isotherms. Moreover we assume no heat flow except that from the earth center.

2.3.1 Model Containing a Spherical Intrusion

In this analysis, we assume a steady flow of heat from the interior to the surface of the earth. For a truly homogeneous and isotropic rock matrix, this heat flow would follow the radial direction of the earth as long as the region of observation is far enough below the surface so that topography will not have a measurable influence on the isotherms (Figure 2-1). Furthermore the undisturbed heat flow is considered unidirectional. If we assume a sphere of thermal conductivity κ, embedded in the matrix rock of thermal conductivity κ (Figure 2-2) then, according to H. S. Carslaw and Y. C. Yaeger[2], the temperature distribution in the matrix is given by

$$T_{(r)} = T_o + GZ \frac{(\kappa - \kappa_1)}{(2\kappa + \kappa_1)} \left(\frac{a^3}{r^3}\right) \quad (1)$$

In this equation:

T_o = rock temperature on a horizontal line through the center of the sphere of radius a.

G = the thermal gradient in the undisturbed matrix rock

Z = vertical distance over the centerline of the point at which $T_{(r)}$ is measured

a = radius of sphere

r = = distance of measuring point to center of sphere

= thermal conductivity of interior of sphere

= thermal conductivity of matrix

$T_{(r)}$ = temperature measured at point given by radius vector r.

The temperature distribution consists of the undisturbed part $T_{(r)} = T_o + GZ$ and the perturbation term

$$T_{(p)} = GZ \frac{(\kappa - \kappa_1)}{(2\kappa + \kappa_1)} \left(\frac{a^3}{r^3}\right) \quad (2)$$

which is the part yielding the temperature variation.

2.3.1.1 Location of Maximum Temperature Change

Figure 2-4 shows a schematic of the model of the tunnel, with obstacle and measurement points. The maximum change in temperature occurs for the condition

$$\frac{\partial^2 (T_{(p)})}{\partial S^2} = 0 = 2\ G\ (a^3) \left(\frac{\kappa - \kappa^1}{2\kappa + \kappa^1}\right) \frac{\partial^2}{\partial S^2} \left(\frac{1}{r^3}\right) \quad (3)$$

where S is defined in Figure 2-4.

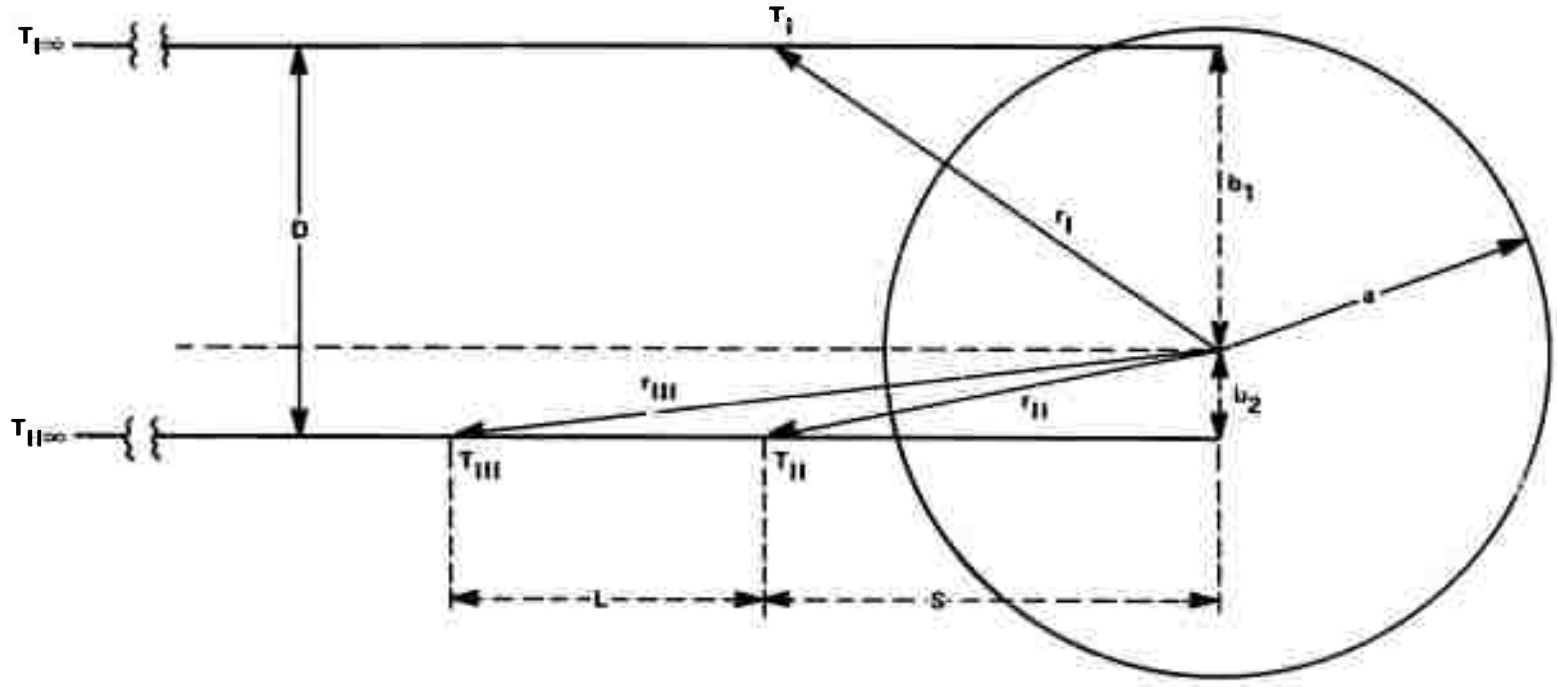

D = DIAMETER OF MINE SHAFT

a = RADIUS OF "OBSTACLE"

$T_I; T_{II}; T_{III}$ = MEASURED TEMPERATURES

$r_I; r_{II}; r_{III}$ = DISTANCE OF LOCATIONS OF T FROM CENTER OF OBSTACLE

$b_1; b_2$ = ECCENTRICITY OF TEMPERATURE LOCATIONS

$T_{I\infty}; T_{II\infty}$ = UNDISTURBED TEMPERATURES

S = DISTANCE OF PLANE $T_I; T_{II}$ FROM CENTER OF OBSTACLE

L = DISTANCE BETWEEN $T_I; T_{II}$ AND T_{III}

P-46-1035-1

Figure 2-4 - Geometrical Layout of Tunnel, Obstacle, and Temperature Measuring Points

$$\frac{\partial^2}{\partial S^2}\left(\frac{1}{r^3}\right) = 0 \tag{4}$$

Considering that

$$r = (Z^2 + S^2)^{1/2}$$

we obtain

$$\frac{\partial^2}{\partial S^2}\left(\frac{1}{r^3}\right) = 0 = -3\,\frac{(Z^2 - 4S^2)}{(Z^2 + S^2)^{1/2}} \tag{5}$$

which yields:

$$Z = +2S$$

for maximum change of temperature as a function of S. This means that those points at which the optimum temperature change occurs are all on a cone formed by straight lines with a slope of ± 2 having their origin in the center of the sphere (Figure 2-5). The axis of rotation is in the vertical direction. Only in special cases will the temperature measurement occur on these cones of maximum temperature change, but then they yield information about the location of the center of the sphere. If we assume that the tunnel head should not be closer than 1.5 times the sphere radius from the center of the sphere before the obstacle is detected, and one still wants to pick up the point at which the optimum temperature change occurs, then we find:

$$x \geq -\frac{b}{a} \pm \left(3^2 - \frac{4b^2}{a^2}\right)^{1/2} \quad \text{with:} \quad b^2 + S^2 = 1.5^2\,(a^2)$$

$$(b + D) \geq 2S \tag{6}$$

$$D = ax$$

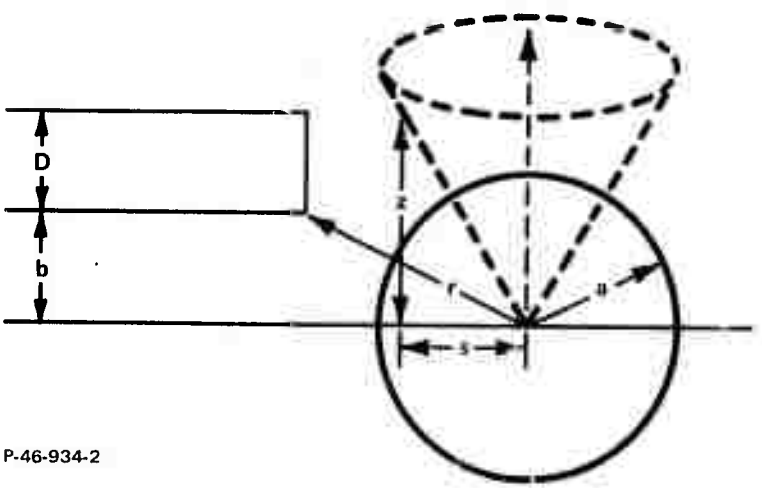

Figure 2-5 - Location of Points of Optimum Temperature Change

Equation (6) simply describes a region of tunnel diameters as a function of b for which the tunnel will intercept the cone of highest temperature change. In reality, this condition is an exception rather than the rule.

2.3.1.2 Temperature Variation as Function of Wall Thickness Between Tunnel and Inclusion

It was shown before that the mathematical term causing the temperature variation T in the case of a spherical inclusion is:

$$\Delta T = G\, b\, \frac{(\kappa - \kappa_1)}{(2\kappa - \kappa_1)} \left(\frac{a^3}{r^3}\right) \qquad (7)$$

Since the values for κ and κ_1 must be assumed, they are chosen for two extreme cases, namely, $\kappa >> \kappa_1$ and $\kappa_1 >> \kappa$. We assume for simplicity's sake that the tunnel floor is on the centerline and thus b = D with D = 2m and $G = 2 \times 10^{-2} \frac{°C}{m}$. If we let a/r = x, then for the spherical case:

$$\Delta T = -2\ (2)\ (10^{-2})\ x^3 = -4 \times 10^{-2}\ x^3\ ,\ \text{for } \kappa_1 >> \kappa \qquad (8)$$

$$\Delta T = +2\ \frac{2}{2}\ (10^{-2})\ x^3 = 2 \times 10^{-2}\ x^3,\ \text{for } \kappa >> \kappa_1 \qquad (9)$$

In Table 2-1, the ΔT is given as a function of percent wall thickness with respect to the cavity radius.

Table 2-1 - Temperature Values for Spherical Model

ΔT (°C)		% Wall Thickness
$\kappa_1 >> \kappa$	$\kappa >> \kappa_1$	
4×10^{-2}	2×10^{-2}	0%
3×10^{-2}	1.5×10^{-2}	10%
2.3×10^{-2}	1.15×10^{-2}	20%
1.8×10^{-2}	0.93×10^{-2}	30%
1.46×10^{-2}	0.73×10^{-2}	40%
1.18×10^{-2}	0.59×10^{-2}	50%
0.98×10^{-2}	0.49×10^{-2}	60%
0.81×10^{-2}	0.405×10^{-2}	70%
0.68×10^{-2}	0.34×10^{-2}	80%
0.58×10^{-2}	0.29×10^{-2}	90%
0.50×10^{-2}	0.25×10^{-2}	100%

From this table, it is clear that the temperature change is detectable under the assumed conditions. If we look at a more realistic case, for example, quartzite in granite then with:

$$\kappa \approx 7 \times 10^{-3} \text{ cal cm sec °C - Quartzite}$$

$$\kappa_1 \approx 10 \times 10^{-3} \text{ cal cm sec } ^\circ\text{C} - \text{Granite}$$

$$\frac{\kappa_1 - \kappa}{\kappa_1 + \kappa} = 0.1765 \text{ and } \frac{\kappa - \kappa_1}{2\kappa + \kappa_1} = 0.111$$

all temperatures are smaller. In Table 2-1, the ΔT in the $\kappa_1 >> \kappa$ column would have to be multiplied by 0.111, that is, the detected temperatures would be only about 1/10 of the values in the table. In the $\kappa >> \kappa_1$ column, the detected temperatures would be 2/10 of the values in the table. It should be pointed out that the case $\kappa_1 << \kappa$ could represent a fracture zone. However, it is hard to estimate the true value of κ_1 in such a fracture zone.

2.3.1.3 Temperature Determination for the Case in Which the Tunnel and the Inclusion Have Equal Dimensions

Here we discuss the situation when the tunnel is of the same diameter as the sphere. We assume that the temperature is monitored close to the tunnel ceiling, so that the point at which the temperature is taken is a distance D/2 away from the center line. That means D/2 = b. We assume further that it is safe to come as close as 1.5 radius to the center of the sphere, thus leaving 0.5 radius of rock between the sphere and the tunnel head.* If at the same time the centerline of the sphere is also D/2 over the tunnel floor, then the temperatures monitored at the ceiling and the floor will have changed by

$$\Delta T_{\text{ceiling}} = 0.125 \; G \; D \; \frac{(\kappa - \kappa_1)}{(2\kappa + \kappa_1)} \qquad (10)$$

*This means r = 2 (1.58)

$$\Delta T_{floor} = -0.125\ G\ D\ \frac{(\kappa - \kappa_1)}{(2\kappa + \kappa_1)}$$

With

$$G = 2 \times 10^{-2}\ °C/m$$

$$D = 2\ m$$

$$\kappa_1 = 2\kappa \text{ (which is realistic)}$$

we get

$$\Delta T_{ceiling} = -1.25 \times 10^{-3}\ °C$$

$$\Delta T_{floor} = 1.25 \times 10^{-3}\ °C \qquad (11)$$

If the tunnel floor is exactly on the sphere's centerline [r = a (1.8)] and all other parameters are the same, then the temperature change at the ceiling is

$$\Delta T_{ceiling} = 1.7 \times 10^{-3} °C \qquad (12)$$

In the case in which the tunnel passes by the sphere with radius a = D at a distance of 0.5 radius above the sphere, floor temperature will show a change of

$$\Delta T_{floor} = 2.2 \times 10^{-3} °C \qquad (13)$$

and at the ceiling it will be a maximum of

$$\Delta T_{ceiling} = 8 \times 10^{-4} °C \qquad (14)$$

All of these values are out of the sensitivity range of present-day instrumentation.

Another case of interest is that of a very large sphere which could either be a volcanic intrustion or a large ore body. If a = 10 x D = 20 m, if the tunnel ceiling is the tangent to the sphere, and if r = 14.15 x D, then

$$\Delta T_{ceiling} = 3.54 \times 10^{-2} °C$$

A change of this magnitude can be detected. For a fracture zone of the same size, we would have $\kappa_1 << \kappa$ and the temperature change would be twice the value above:

$$\Delta T_{ceiling} = 7.08 \times 10^{-2} °C \qquad (15)$$

Thus, inclusions of this magnitude can be sensed.

We did show, however, that hazardous conditions can exist which do not give a strong enough signal to be detected. Thus, when the first signal changes occur, one has to expect the least favorable situation, and assume that a relatively small though hazardous disturbance lies ahead of the tunnel face. Thus, precautions would have to be taken.

2.3.1.4 Analytical Determination of the Location of the Obstacle

In practice, it is highly desirable to know the size and location of an obstacle. This makes it necessary to solve the set of equations for the size and the exact location of the sphere given below. This is done here for a two-dimensional model, in which the sphere's cross section and one tunnel wall are in the same plane. The geometrical relations are shown in Figure 2-4. The set of equations to be solved for S, a, $(\kappa - \kappa_1)/(2\kappa + \kappa_1)$, and b, is:

$$T_I = T_c + b_1 G \left[1 + \frac{(\kappa - \kappa_1)}{(2\kappa + \kappa_1)} \left(\frac{a^3}{r_I^3}\right)\right] \tag{16}$$

$$T_{II} = T_c + b_2 G \left[1 + \frac{(\kappa - \kappa_1)}{(2\kappa + \kappa_1)} \left(\frac{a^3}{r_{II}^3}\right)\right] \tag{17}$$

$$T_{III} = T_c + b_2 G \left[1 + \frac{(\kappa - \kappa_1)}{(2\kappa + \kappa_1)} \left(\frac{a^3}{r_{III}^3}\right)\right] \tag{18}$$

$$T_{IV} = T_c + b_1 G \left[1 + \frac{(\kappa - \kappa_1)}{(2\kappa + \kappa_1)} \left(\frac{a^3}{r_{IV}^3}\right)\right] \tag{19}$$

$$r_I = S^2 + b_1^2 \; ; \quad r_{II} = S^2 + b_2^2 \tag{20}$$

$$r_{III} = (S + \ell)^2 + b_2^2 \; ; \quad r_{IV} = (S + \ell)^2 + b_1^2 \tag{21}$$

$$D = b_1 - b_2 \; ; \quad \frac{(\kappa - \kappa_1)}{(2\kappa + \kappa_1)} a^3 = A^3 \tag{22}$$

$$T_{I\infty} = T_c + G\, b_1$$

It turns out that $\frac{(\kappa - \kappa_1)}{(2\kappa + \kappa_1)}$ and "a" cannot be separated. Only a value

$$A^3 = \frac{(\kappa - \kappa_1)}{(2\kappa + \kappa_1)} a^3$$

the "effective radius" can be determined. The reduced equations to be solved for the unknowns b_1, A, and S are

$$\frac{T_I - T_{I\infty}}{V} = \frac{b_1 A^3}{\left(S^2 + b_1^2\right)^{3/2}} \tag{23}$$

$$\frac{T_{II} - T_{I\infty} + VD}{V} = \frac{(b_1 - D) A^3}{\left[S^2 + (b_1 - D)^2\right]^{3/2}} \tag{24}$$

$$\frac{T_{III} - T_{I\infty} + VD}{V} = \frac{(b_1 - D) A^3}{\left[(S + \ell)^2 + (b_1 - D)^2\right]^{3/2}} \tag{25}$$

The solution of these equations requires an iteration program on a computer. After a program was written for this problem, the evaluation of the temperature measurements yielded 4 solutions for each set of three temperatures.

In the following, a numerical example is given in which the first set of temperatures at locations I, II, and III were calculated for given values of $T_{I\infty}$, V, D, κ_1, a, b_1, b_2, S, ℓ, κ For an example, the data used are:

$$T_{I\infty} = 20°C$$

$$V = 1.8 \times 10^{-2} °C/meter$$

$$D = 1.5 \text{ meters}$$

$$\kappa = 10,\ \kappa_1 = 7;\ \frac{(\kappa - \kappa_1)}{(2\kappa + \kappa_1)} = \frac{1}{9}\ ;\ A^3 = \frac{(\kappa - \kappa_1)\ (1)^3}{(2\kappa + \kappa_1)}\ ;\ A = \frac{1}{\sqrt[3]{9}} = 0.48$$

$$a = 1 \text{ meter}$$

$$b_1 = 1.0 \text{ meter}$$

$$b_2 = 0.5 \text{ meter} \; ; \; b_1 = D + b_2; \; b_2 = b_1 - D$$

$$S = 1.5 \text{ meters}$$

$$\ell = 1 \text{ meter}$$

From these values we calculated the temperatures T_I, T_{II}, T_{III} and used them in the computer program to calculate the unknowns S_1, b_1, b_2, A. The program gave the following four solutions given in Table 2-2.

Table 2-2 - Calculation of Unknowns

	I	II	III	IV
S	-0.383	0.020	0.7417	1.5
b_1	1.48	0.694	0.499	1.0
b_2	0.02	-0.806	-1.001	-0.5
A	0.383	0.209	0.3005	0.4807

Obviously the data in the fourth column are the right solutions. In practice however, one would not know this and all solutions would have to be considered.

The solutions in column I imply that we have already penetrated the obstacle and that the location of T_I and T_{II} measurement is beyond the center of the sphere. These solutions can be excluded since another temperature change would have been observed before the obstacle was penetrated and a change in rock formation would have been detected. So, although the solution is valid physically and mathematically, it is not realistic.

The solutions in the second column mean that "a" is smaller than 0.020 m which is unrealistic.

The third solution requires that

$$0.3005 - 2^3 \frac{(\kappa - \kappa_1)}{(2\kappa + \kappa_1)} \tag{26}$$

Since S = 0.74 m, the radius "a" could be of that same order if the ratio of κ/κ_1 turns out to be realistic. In order to check this, Equation (26) is solved for $\kappa = k\,\kappa_1$. Thus

$$\frac{(0.3005)^3}{(0.7417)^3} = 6.4 \times 10^{-2} = \frac{(\kappa - \kappa_1)}{(2\kappa + \kappa_1)}$$

when solved for κ, this equation yields

$$\kappa = 1.22\,\kappa_1$$

This is a realistic case. It means that $\kappa_1 < \kappa$ which could occur in a fracture zone. So this solution is possible, although it is not the one we used to calculate T_I, T_{II}, and T_{III}. This shows that one set of T_I, T_{II}, T_{III} measured in a tunnel would give up to four solutions for the location and the effective size of the obstacle. Moreover, the observer cannot always distinguish between the purely mathematical and the real solution.

2.3.1.5 Determination of Error in Location Due to Temperature Error

In order to obtain information about the size of the error in the calculation of the coordinates and the "effective radius" of a spherical inclusion, the example calculated before was again solved for the two cases in which the temperatures T_I, T_{II}, and

T_{III} were changed by $\pm 0.005°C$. This deviation of 0.005°C is on the order of the resolution of the radiometer and will certainly occur. Table 2-3 gives the results for these two cases. Again four solutions are obtained, but none is even close to the data used in the previous exact calculation.

Table 2-3 - Effect of Temperature Measurement Error on Calculated Coordinates

$\Delta T_I = +0.005°C$

B_1	S	A
23.31	5.95	5.36
1.55	-0.497	--
-10.93	77.8	--
-0.174×10^{-4}	79.77	1963.0

$\Delta T_I = -0.005°C$

1.54	-0.50	0.936
12.54	-74.26	21.62
-0.1149×10^{-4}	-75.89	--
-20.4	-7.52	5.3

This means that any temperature deviation on the order of $5 \times 10^{-3}°C$ will make the prediction of both the location and the effective radius "A" impossible for changes in geological dimensions on the order of meters. It also has to be borne in mind that, in reality, the areas of geological change rarely if ever have the shape of a true sphere. For irregular shapes, no mathematical model would have any general value.

2.3.2 Model Containing an Area of Cylindrical Shape

For a geological change of cylindrical shape and infinite length, the term introducing the temperature change into the otherwise undisturbed temperature field outside the cylinder is:

$$\Delta T = \frac{(\kappa - \kappa_1)}{(\kappa + \kappa_1)} \; G \; Z \; \frac{a^2}{r^2} \quad : \qquad (27)$$

$$z = D$$

for $G = 2 \times 10^{-2}$°C/m, $\kappa_1 = 2\kappa$

$$\Delta T = \frac{2 \times 10^{-2}}{3} \quad \frac{a^2}{r^2}$$

If we again assume that we would like to detect the change in temperature for a cylinder of a = 2m, a tunnel diameter of D = a, and tunnel face 1.5 (a) away from the cylinder then

$r = a\sqrt{3.25}$ and Equation (27) yields

$$\Delta T = 4.1 \times 10^{-3}\text{°C}$$

This is again smaller than the sensitivity of existing radiometers, if the measurement is supposed to predict hazards. In principle, the same rules apply for the location and the size of the sphere, as were the case for the solution of the spherical case. Therefore a detailed evaluation by computer was not performed.

2.3.3 Temperature Variation as a Function of Wall Thickness Between Tunnel and Inclusion

The mathematical term causing the temperature variation ΔT in the case of a cylindrical inclusion is

$$\Delta T = Gb \frac{(\kappa_1 - \kappa)}{(\kappa_1 + \kappa)} \left(\frac{a^2}{r^2}\right) \qquad (28)$$

Since the values for κ and κ_1 must be assumed, they are again chosen for two extreme cases, namely, $\kappa >> \kappa_1$ and $\kappa_1 >> \kappa$. We further assume for simplicity's sake that the tunnel floor is on the centerline; thus, $b = D$ with $D = 2m$ and $G = 2 \times 10^{-2}$°C/m. If we let $a/r = x$ then for the cylindrical case:

$$\Delta T = \pm 4 \times 10^{-2} x^2 \tag{29}$$

The values of ΔT as a function of the percent wall thickness with respect to the inclusion radius are given in Table 2-4.

Table 2-4 - Temperature Values for Cylindrical Model

ΔT (°C)	Wall Thickness
4×10^{-2}	0%
3.3×10^{-2}	10%
2.8×10^{-2}	20%
2.35×10^{-2}	30%
2.64×10^{-2}	40%
1.78×10^{-2}	50%
1.56×10^{-2}	60%
1.38×10^{-2}	70%
1.24×10^{-2}	80%
1.11×10^{-2}	90%
1.00×10^{-2}	100%

If instead of the assumed values for κ and κ_1, we again use more realistic values

$$\kappa = \frac{10}{7} \kappa_1$$

then all the temperature values would decrease by one order of magnitude and their detection would not be possible.

2.3.4 Summary of Mathematical Analysis

In summary, it can be said that hazard prediction using temperature monitoring in tunnels cannot be achieved in all cases. Only for geological changes of large size - many times the size of the tunnel - can temperature changes be expected which are of a size large enough to be observed with certainty.

Other factors which have an influence on the temperature measurements are the presence of heat-dissipating machinery, heat-producing excavation processes, the presence of moisture, the possible masking effect of thin layers of dust, and the heat exchange with the air in the tunnels. These influencing factors were examined experimentally and will be discussed in Section 4.

2.4 A URANIUM ORE BODY AS A MODEL OF A GEOTHERMAL SOURCE

Uranium is known to exhibit radioactive decay. This means that energy is released from the uranium ore bodies into the matrix rock in which the ore is embedded. As a simple model, we will again assume a large spherical ore body 20 m in diameter, in order to estimate the temperatures to be expected outside the sphere at a distance of a few meters from the sphere's surface. This model was chosen since uranium mines seemed to be the only mines with geothermal action that were accessible for measurements. Due to company policies of the various mines, however, we could not obtain permission to perform measurements in the mines useful for our purposes.

In order to calculate the temperatures, we assume that all energy released during a radioactive decay is completely converted into heat. This seems reasonable because of the fact that the uranium atoms are completely surrounded by large masses of other atoms of the elements which make up the matrix rock. The data used were taken from the Handbook of Physics and Chemistry. Table 2-5 gives the 3 occurring uranium isotopes, their abundance, and their half-life.

Table 2-5 - Properties of Uranium Isotopes

Isotope	Abundance = A_n	Half-Life = τ_n
U^{234}	5.7×10^{-5}	2.48×10^{5} years
U^{235}	7.2×10^{-3}	7.13×10^{8} years
U^{238}	9.9×10^{-1}	4.51×10^{9} years

The decay processes leading to emission of particles and their dissipating energy are listed in Table 2-6. The energy released per unit time by one isotope is: $E_{av} \times dN_n/dt$ with

$$\frac{dN_n}{dt} = k_n (N_n)$$

$$k_n = \frac{\ell n_2}{\tau_n}$$

where N_n is the number of atoms of isotope n and k_n is the decay constant of isotope n. The average energy E_{av} is determined as

$$E_{av} = \sum_{\ell} E_e \alpha_e \qquad (30)$$

Table 2-6 - Uranium Decay Processes

Isotope	Relative Distribution of Emission Process α_e	Emergy MeV Emitted
U^{234}	0.72	4.77
	0.28	4.72
U^{235}	0.067	4.559
	0.25	4.370
	0.35	4.354
	0.14	4.333
	0.08	4.318
	0.058	4.117
U^{238}	0.77	4.195
	0.23	4.14

with E_e the energy released by a decay process times the probability α_e of this particular process. Therefore, the total energy released per unit time by a sample of N uranium atoms containing amounts of all isotopes according to their natural abundance is

$$\frac{dE}{dt} = \sum_n E_{av_n} k_n N_n \tag{31}$$

Since the total number of atoms is N, one finds

$$N_n = N A_n$$

Thus

$$\frac{dE}{dt} = N \sum E_{av_n} k_n A_n \tag{32}$$

or

$$\frac{dE}{dt} = N \sum_{n} A_n k_n \sum_{\ell} \alpha_\ell E_\ell \qquad (33)$$

or with $A_n k_n \sum_{\ell} E_\ell \alpha_\ell = \frac{dE_n}{dt}$ and n = 3 the number of isotopes, one finds

$$\text{for } U^{234}: \quad \frac{dE_I}{dt} = 7.55 \times 10^{-10} \ \frac{MeV}{year}$$

$$\text{for } U^{235}: \quad \frac{dE_{II}}{dt} = 2.16 \times 10^{-11} \ \frac{MeV}{year}$$

$$\text{for } U^{238}: \quad \frac{dE_{III}}{dt} = 6.4 \times 10^{-11} \ \frac{MeV}{year}$$

This leads to

$$\sum_{n} A_n k_n \times \left(\sum_{\ell} E_\ell \alpha_\ell \right) = \sum_{n} \left(\frac{dE_u}{dt} \right) \approx 8.4 \times 10^{-10} \ \frac{MeV}{year} \qquad (34)$$

The total energy dissipated from a sample of N atoms is:

$$\frac{dE}{dt} = N \times 8.4 \times 10^{-10} \left[\frac{MeV}{year} \right] = N \times 4.25 \times 10^{-30} \ [W] \qquad (35)$$

If N is the number of atoms per cubic centimeter of ore, then $\frac{dE}{dt}$ is the energy released in one cm^3 per second or W/cm^3. Assuming the ore contained 0.06 percent uranium, then under the assumption that one cm^3 contains 10^{22} Atoms

$$N = 6 \times 10^{18}$$

Thus the power generated in 1 cm^3 is

$$\frac{dE'}{dt}\left[\frac{W}{cm^3}\right] = 6 \times 4.25 \times 10^{-12}\left[\frac{W}{cm^3}\right] = 2.55 \times 10^{-11}\left[\frac{W}{cm^3}\right] \qquad (36)$$

If one now assumes an ore body of spherical shape with a diameter of 20 m, then the energy flux at the surface of this sphere would be:

$$\frac{dE'}{dt} \times \frac{\text{Volume of sphere}}{\text{Surface area of sphere}} = \frac{dE^*}{dt}$$

$$\frac{dE^*}{dt} = \frac{dE'}{dt}\left(\frac{4\pi r^3}{3}\right)\left(\frac{1}{4\pi r^2}\right) = \frac{dE'}{dt}\left(\frac{r}{3}\right) \qquad (37)$$

with $r = 10^3$ cm.

$$\frac{dE^*}{dt} = 2.55 \times 10^{-11}\left(\frac{10^3}{3}\right) = 8.5 \times 10^{-9}\left[\frac{W}{cm^2}\right]$$

If the matrix rock in which the uranium ore sphere is embedded consists of gneiss with a thermal conductivity $\kappa = 7 \times 10^{-3}\left[\frac{cal}{°C - cm - sec}\right]$, the thermal gradient at the surface of the sphere is:

$$\frac{dT}{dx} = \frac{1}{\kappa}\left(\frac{dE^*}{dt}\right)\left[\frac{cal}{sec - cm^2}\right] \qquad (38)$$

$$\frac{dT}{dx} = \frac{4.19\ (8.5 \times 10^{-9})}{7 \times 10^{-3}} = 5.07 \times 10^{-6}\left[\frac{°C}{cm}\right]$$

or

$$\frac{dT}{dx} = 5.07 \times 10^{-4} \left[\frac{°C}{cm}\right]$$

This gradient is not within the sensitivity range of our instrumentation. If the ore concentration is one order of magnitude higher, then under very favorable conditions, one might be able to detect a temperature signal.

SECTION 3

INSTRUMENTATION SELECTION

3.1 TEMPERATURE MEASURING INSTRUMENT AND PROCEDURE

Factors considered in the selection of a particular infrared radiometer as the most favorable instrument for temperature measurements were the following:

- The accessibility of locations at which temperatures are to be measured.
- The fact that a thermocouple probe undesirably interacts with rocks.
- The possibility that temperatures may be averaged over areas from a few square inches to a few square feet.
- Mine environmental conditions in mines like humidity, dust, and sometimes low ambient temperatures.

Based on these selection factors, the Barnes precision Radiation Thermometer Model PRT-5 was chosen; this instrument performed well under all conditions encountered during the experimental part of the project. Originally the Barnes 12-511 radiometer was chosen, but it did not perform reliably in laboratory tests at temperatures around 20°C or below.

The method utilized in temperature measurements with a radiometer is based on the fact that a body emits radiation with a spectral distribution that depends on the temperature and emissivity of that body. For a so-called black body, the spectral radiance (radiant power per unit projected target area per unit solid angle per unit wavelength interval) is given by the Planck radiation function

$$N_{b\lambda} = C_1 \left(\pi^{-1}\right) \left(\lambda^{-5}\right) \left(e^{C_2/\lambda T} - 1\right)^{-1} \qquad (39)$$

where

$N_{b\lambda}$ = spectral radiance of a black body

C_1 = the first radiation constant

C_2 = 0.014388 (M°K) the second radiation constant.

λ = wavelength of radiation

T = absolute temperature of the black body.

The ideal black-body radiance is modified however by the emissivity $\varepsilon(\lambda)$ of the body of interest, thus leading to real radiance of

$$N_\lambda = \varepsilon(\lambda)\ N_{b\lambda} \tag{40}$$

In order to be detected, this radiation has to travel through the atmosphere from the target to the detector, so that its spectral distribution is changed by selective absorption of radiation by H_2O, O_2, and CO_2. The detection of this radiation also depends on the spectral response of the detector. These difficulties can be avoided by selective detection in a relatively small range of wavelengths.

It turns out that for the temperature range of 32° to 100°F, the maximum spectral radiance occurs around λ = 10μm. This also happens to be a wavelength range in which almost no absorption occurs in the air[3]. Thus by selecting the right kind of infrared optics and detector, the total radiance detected can be limited to

$$N = \int_{\lambda_1}^{\lambda_2} \varepsilon(\lambda)\ N_b\ (\lambda,\ T)\ d\lambda \tag{41}$$

For the Barnes PRT-5, λ_1 = 8 μm and λ_2 = 14μm.

The detector in this instrument is a thermistor bolometer whose spectral response is flat between $8 \leq \lambda \leq 14\mu m$, and the lens forming the image of the target area on the detector is a 10 mm f/2.8 made from IRTRAN-2. The spectral passband of the lens covers the range from 0.6μm to 14μm. The 8μm cutoff is produced by an interference filter.

Based on the information above, the PRT-5 was chosen as a suitable instrument for this project. Aside from the performance considerations, the PRT-5 is also light, compact and thus easy to handle.

According to the PRT-5 manual, the accuracy of the instrument is $0.5^{o}C$ absolute temperature, but this number is not of great importance, since in the present application only temperature changes are of interest. The sensitivity of the PRT-5 is $0.1^{o}C$ for the meter readout and about $0.004^{o}C$ on the recorder output. The recorder output was used throughout the experimental part of this program, since it alone provided the sensitivity to detect the temperature changes caused by geological changes in rocks. The total noise was on the order of $0.007^{o}C$. A measurement duration of about five minutes was sufficient to integrate out the noise.

The recorder used in conjunction with the PRT-5 was a Hewlett-Packard X-Y recorder. The experimental setup in the mine is shown in Fig. 3-1.

3.2 RADIOMETER CORRECTIONS

Due to the difference between the emissivity of a true black body and that of a real body, a certain error is introduced into the determination of the target temperature. If one assumes that Wien's radiation law is a good approximation to Planck's law in the wavelength region of interest, then the temperature error is

$$\Delta T = -\frac{\lambda T^2}{C_2} \ln(\varepsilon_\lambda) \qquad (42)$$

This means that for a given λ and a given temperature T, the radiometer reading will give a temperature value which is $\Delta T^{o}C$ lower than the actual value. The ΔT for $T = 300^{o}K$ as a function of the emissivity is given in Table 3-1.

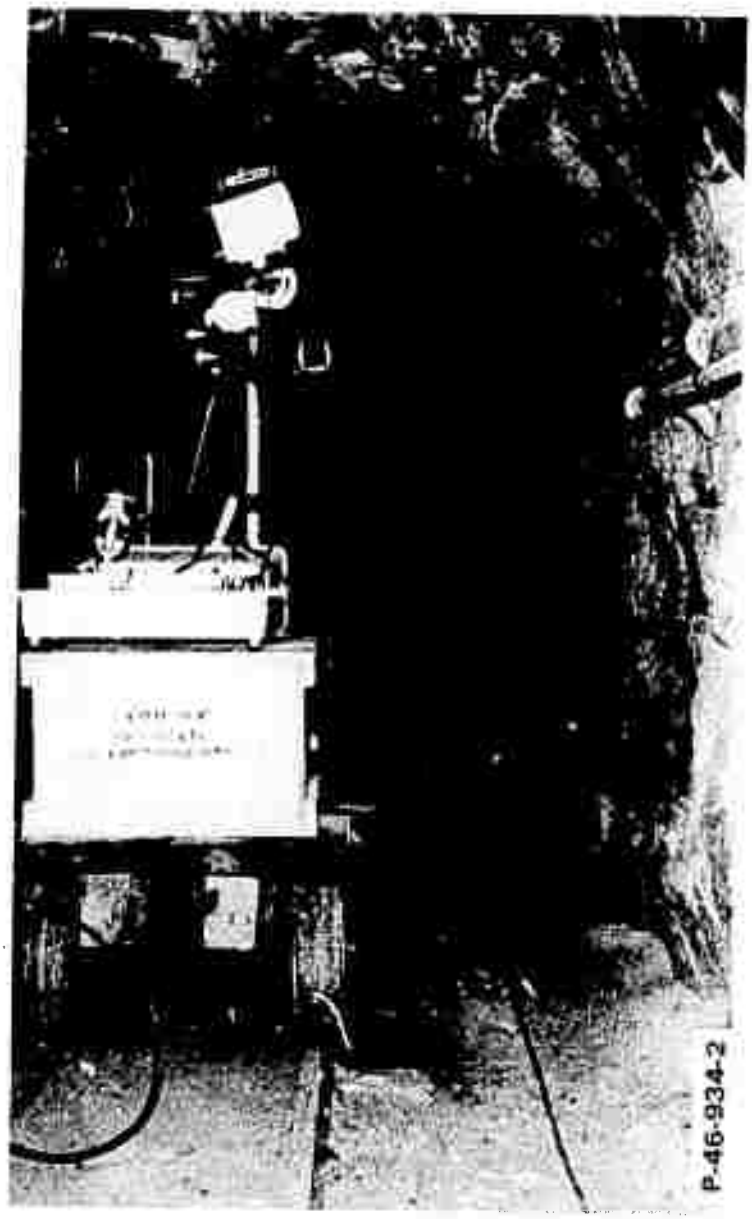

Figure 3-1 - Experimental Setup in The Mine

Reproduced from best available copy.

Table 3-1 Temperature Error as a Function of Emissivity

ε_λ	ΔT
0.9	$\sim 6.7^\circ C$
0.8	$\sim 14.0^\circ C$
0.7	$\sim 22.4^\circ C$
0.6	$\sim 32.0^\circ C$
0.5	$\sim 43.2^\circ C$
0.4	$\sim 57.3^\circ C$

$\lambda = 10\mu m = 10^{-5} m$

$T = 300^\circ K$

$C_2 = 0.014388\ m\ ^\circ K$

This shows that a change in emissivity of 10% can cause an error of several degrees Centigrade. If the measurements are performed on a perfectly homogeneous rock, then only the absolute value of the measured temperature will be off. However, if the rock composition changes drastically from one measuring site to the next, then an unknown error is introduced that can only be completely eliminated by determining the emissivities. However, a drift resembles a black-body radiation cavity as long as no large perturbations are introduced. This effect has to be borne in mind in the evaluation of radiometer measurements.

Another factor important in the evaluation of radiometer temperature measurements of rock materials is the transmittance of materials. If a material is not opaque, radiation will escape from its interior. The location below the surface at which the radiation originates depends on the transmittance or the absorption. In a case in which there is no temperature gradient in this body, the radiation is in equilibrium and there is no effect on the measurement. If, however, the temperature is higher on the inside, then the surface temperature measured will seem higher than that for an opaque material, depending on the transmittance.

Still another phenomenon to consider is the effect of polarization. Normally when one thinks of black-body or "near black-body" radiation, preferential or total polarization[4] of the emitted light is not taken into account. In a real environment, especially in the case of rocks, the material is crystalline and thus the radiation it emits may be polarized. The degree to which polarization occurs depends of course on the types of crystals, the size of these crystals, and also on the frequency with which the various orientations (with respect to the surface)

occur, i.e. whether the crystals occur with a preferential orientation. In intrusions and in banded rocks, this preferential orientation is expected and thus leads to polarization, which in turn leads to a deviation of the radiance from that of a black body. All the above-mentioned effects are known, but no data were found in the literature. The determination of the optical characteristics of rocks requires special equipment and is a rather lengthy research project in itself. To avoid complications due to the lack of information on the optical constants of rock, we performed our measurements in such a fashion that the perturbation was kept as small as possible. This was done by choosing the site of our field tests such that the change of lithology was minimized, or else by testing rock samples in our laboratory for differences in emissivity.

SECTION 4
EXPERIMENTAL FIELD TESTS AND RESULTS

4.1 SITES OF MEASUREMENTS

The objective of the field test of the radiometer was to measure the magnitude of temperature changes due to causes other than inclusions of different lithology. Perturbations were expected from ventilations, radiation sources, and the excavation process itself. Thus, mines with a number of drifts on one level and with adequate control over the ventilation were needed so that experiments could be performed in unventilated drifts. It was also desirable to have blasted as well as bored tunnels available so that the difference in temperature distribution between those two types of tunnels could be observed. Bearing this in mind, different test sites were chosen. The first one was the experimental mine of the Colorado School of Mines in Idaho Springs, Colorado and the second one was an iron ore mine of the Republic Steel Company in Mineville, New York.

The experimental mine of the Colorado School of Mines is located about 7800 feet above sea level and consists of a main tunnel with a number of drifts and chambers. (Fig. 4-1) The entire system of tunnels and drifts is on the same elevation. The rock formation is metamorphic gneiss. The mine is in the flank of a mountain, and therefore topography is probably of influence on the temperature distribution in the rock itself. In spite of a few weathered zones which are wet, the mine is extremely dry. The ventilation system of the mine has its exhaust through a source at the end of the main tunnel and takes in outside air through the main entrance. Due to this arrangement, the temperature in the main tunnel fluctuates with the outside air temperature and with the operation of the ventilator. The drifts are ventilated using small portable blowers only during drilling or after blasting. All drifts of interest had tracks in them so that the radiometer and the recorder

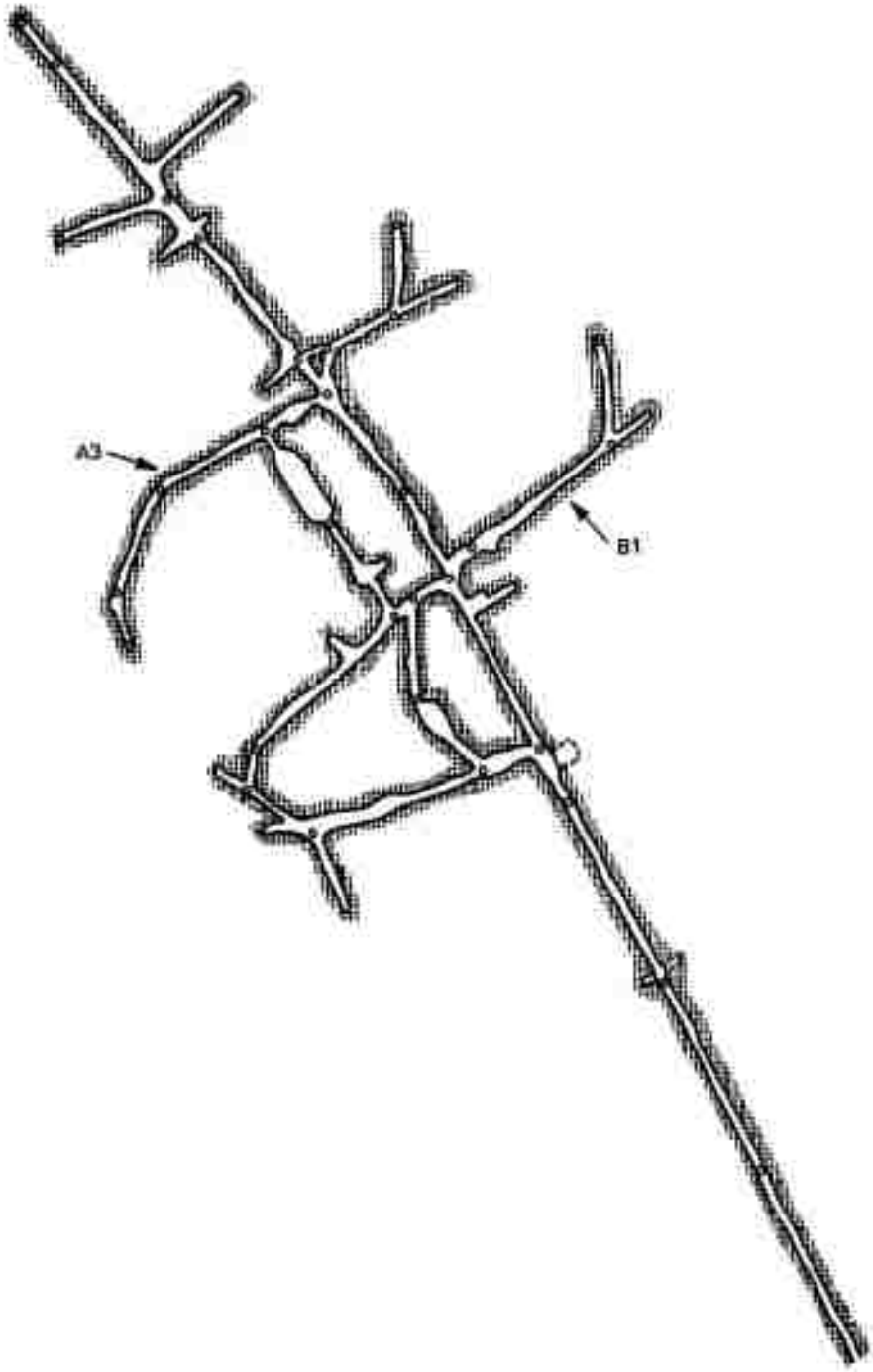

Figure 4-1 - Schematic of the Experimental Mine of the Colorado School of Mines

could be mounted on a flatcar and easily moved. Both 220 and 110 V power supplies were available.

The iron ore mine of the Republic Steel Company is a deep mine extending up to 3200 feet below the surface. The major rock formation is metamorphic gneiss with very large continuous deposits of magnetite. There are some faulted zones, but in general, there are large areas of undisturbed rock. Due to the depths, the influence of the topography in the area is nonexistent.

This mine was of special interest because in 1969 the Army performed heat absorption experiments[5] in one drift. The rock - originally blasted - has spalled off and was stress-relieved with very smooth surfaces exposed. Since these were large areas of solid smooth rock, we assumed that the temperature variation due to loose rock would be almost nonexistent. The measurements revealed no measurable temperature deviation over areas in which we definitely found loose rock. Close inspection showed, however, that the spalling during the Army experiments has left many thin slate-like layers of gneiss and that on a small scale all of the wall consisted, for all practical purposes, of thin slices of loose rock. An investigation with a magnifying glass showed clearly that, apparently due to the heat dissipated into the rocks during the Army experiment, the microstructure of the gneiss was drastically changed. Its mechanical strength was reminiscent of soft sandstone.

Since the ore body in the mine is of large dimensions, it was expected to have a measurable influence on the temperature distribution in the rocks. In addition, the Republic Steel Mine had a site in which a bored tube, 8 feet in diameter, was accessible for temperature measurements. The tube itself penetrated both the ore body and the gneiss and was without any ventilation. (Fig. 4-2). Thermal equilibrium between air and rock was well established since the mine had not been worked for many months. The tube had a slope of 30° and was closed at the deep end.

The Experimental Mine in Colorado was chosen for studies on temperature fluctuations due to perturbations by rock, air, etc., and for studies on the feasibility of measuring inherent rock temperatures immediately after blasting.

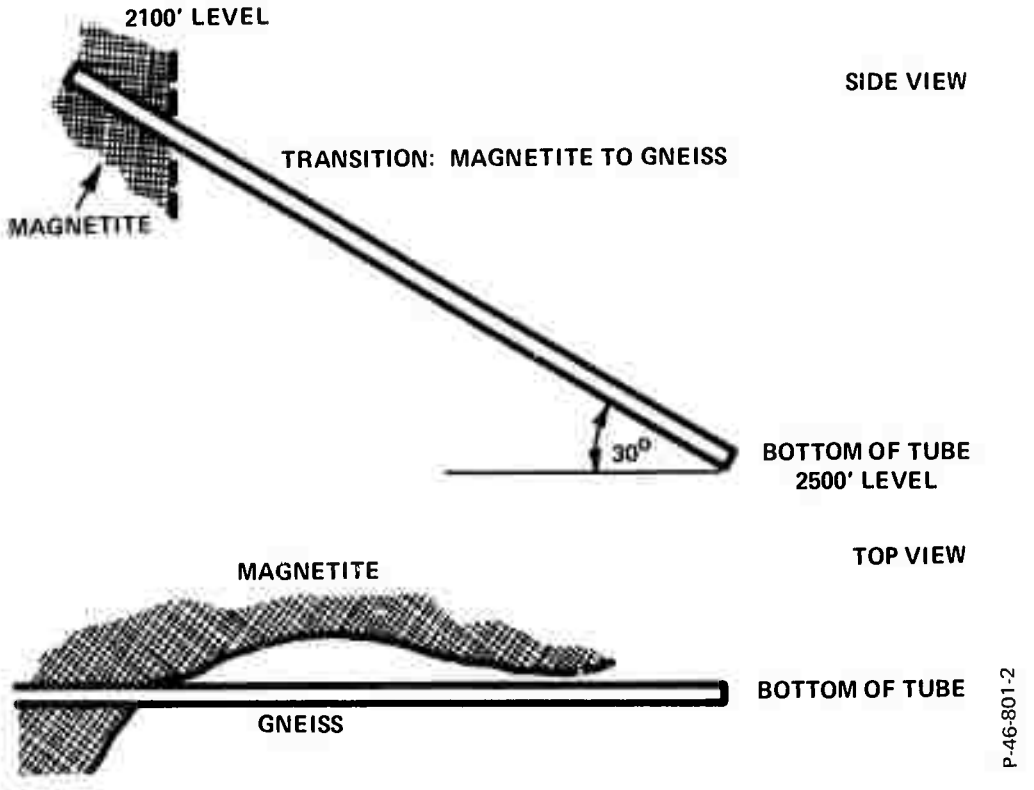

Figure 4-2 - Schematic of Lithology Around Bored Tube

The Republic Steel Mine in Mineville was chosen for studies on the temperature distribution on large areas of undisturbed rock in the vicinity of large ore bodies.

4.1.1 Temperature Measurements on a Rock Surface with an Intrusion as well as Both Heavily Jointed and Solid Regions. (Colorado School of Mines Experimental Mine)

This site was chosen because of its multitude of rock structures exposed in a relatively small area. The area consisted of gneiss with various amounts of biotite, a large feldspar intrusion, a fracture zone, and areas with solid rock, thus offering an opportunity to study the effects of these lithologies on the radiometer temperature measurements.

Figure 4-3 shows the feldspar intrusion in the gneiss matrix. The measuring tape defines a distance of 4-1/2 feet over which sets of radiometer measurements were taken at 3-inch intervals.

Figure 4-3 - Feldspar Intrusion in Geneiss Matrix

Reproduced from best available copy.

The first set of measurements was taken at a distance of 4 inches above the tape going from the left to the right. The changes in temperature are plotted in Fig. 4-4.

The measurements were repeated three times in order to determine their fluctuations. The general trend of all curves plotted shows an apparent increase of temperature while going to the right across the intrusion but were not reproducible in detail. During the measurements, the air temperature was constant, so that fluctuations of the rock temperature could not be attributed to changes in the heat exchange between the rock and the air. Thus, the differences between the three temperature curves must have a different cause. From point 9 on, the rock showed a joint and was fractured and loose. At the same time, however, the composition of the rock was somewhat inhomogeneous over small areas with feldspar and biotite interspersed. Both of these conditions can lead to fluctuations of the signal output from the radiometer.[6] Loose rock can have temperatures different from that of the solid rock matrix. Thus, the fracturing could have caused true temperature variations. The change in composition (dark biotite interspersed in the feldspar) can mean a change in thermal emissivity; if there is an outside radiation source, a change in reflectivity can cause signal fluctuations. It will be shown later than the reflectivity was responsible for the fluctuation in these measurements.

The second scan across the feldspar intrusion is shown in Fig. 4-5. These measurements were made on a horizontal line 8 inches below the first scan. The scans obtained are much smoother, indicating very few abrupt changes in apparent temperature. Again, the general trend is an increase in the apparent temperature while going to the right. The intrusion manifests itself as a hump in the temperature curve. The temperatures measured are, on the average, smaller than those measured above the tape. At points 2 and 3, the apparent temperature even dropped a small amount below that of point 1. Referring to Fig. 4-3 which shows the topography of the rock, one can see a spot

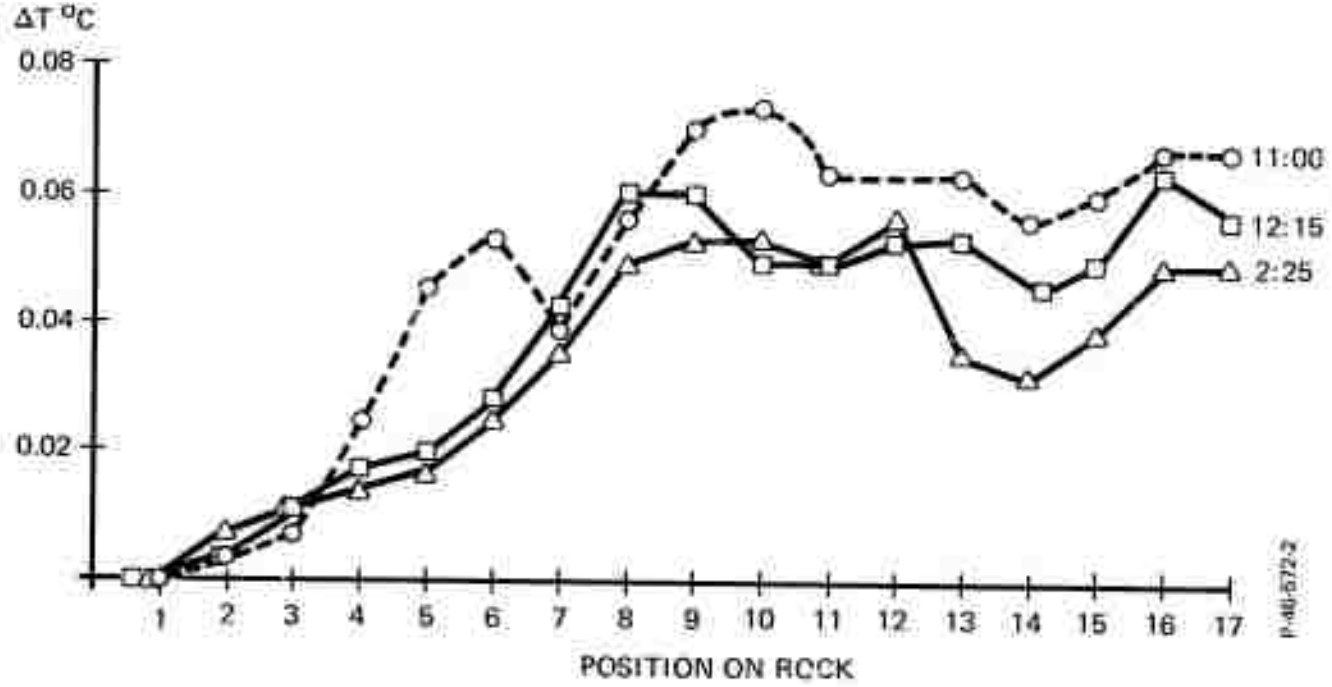

Figure 4-4 - First Sweep Over Feldspar Intrusion

which has a color (actually brown at the test site) different from that of the biotite. This spot covers part of the areas belonging to points 2 and 3. Also at the end (points 16 and 17) the temperature curve goes up, after a slight decline. This coincides with the change of composition in the rock. Both sets of measurements seemed to indicate that the signal obtained with the radiometer was possibly determined by either the emissivity or the reflectivity of the rock rather than by a true temperature variation.

In an effort to determine if reflectivity was the cause of variations, the influence of the incandescent light in the chamber was checked. No detectable effect on the measurements was observed.

The only other radiation sources present were the two operators performing the measurement. The temperature record in Fig. 4-6 shows the difference between three measurements.* At first, 2 persons are standing behind the radiometer about 15 feet away from the chamber wall. After one person leaves, the radiometer signal drops, indicating a temperature decrease of $0.03^{\circ}C$. When the second person leaves, the signal drops another $0.07^{\circ}C$. This clearly indicates that the reflection of body radiation was of great significance in the radiometer measurements. Fig. 4-7 shows a scan across the intrusion corresponding to the first scan above the tape, with no one present during measurements. The temperature variation is much smaller and almost reversed. The dark-colored region gives a larger signal than the lighter one, which is probably due to the difference in emissivity. The fact that fluctuation of the signal is still more than $1 \times 10^{-2}{}^{\circ}C$ is rather significant, considering that the experiment was intended to measure temperature changes of this same order of magnitude for the prediction of hazardous geological changes ahead of tunneling operations.

Temperatures in the vertical direction fluctuated by about the same magnitude. However, temperatures measured about 1 foot above the floor were generally $0.02^{\circ}C$ lower. This means that the rock temperature

*Taken at point 9 on lower line.

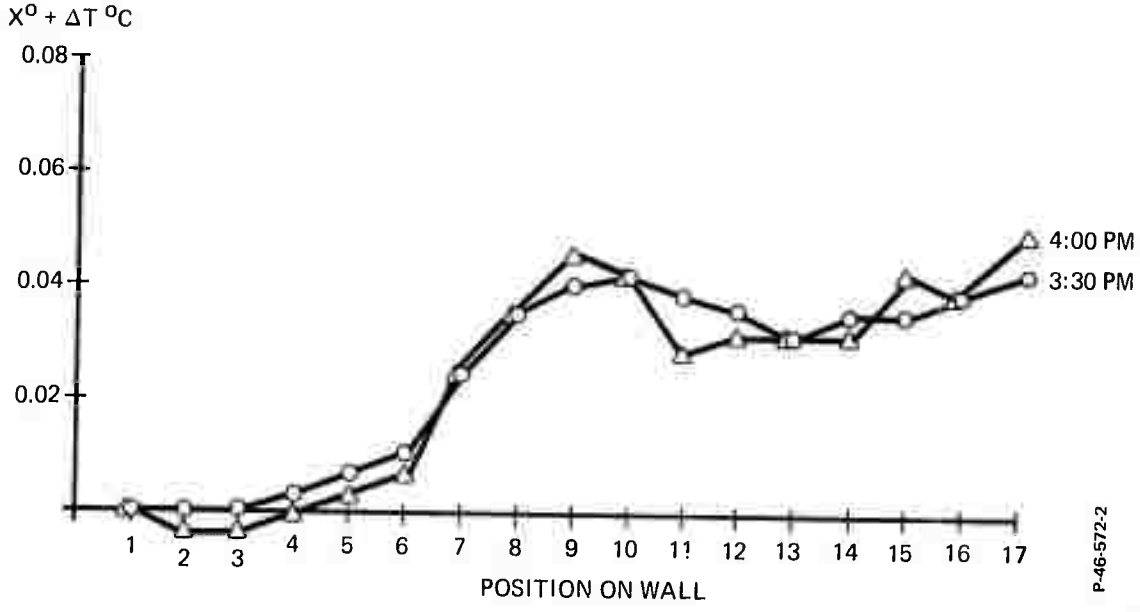

Figure 4-5 - Second Scan Over Feldspar Intrusion

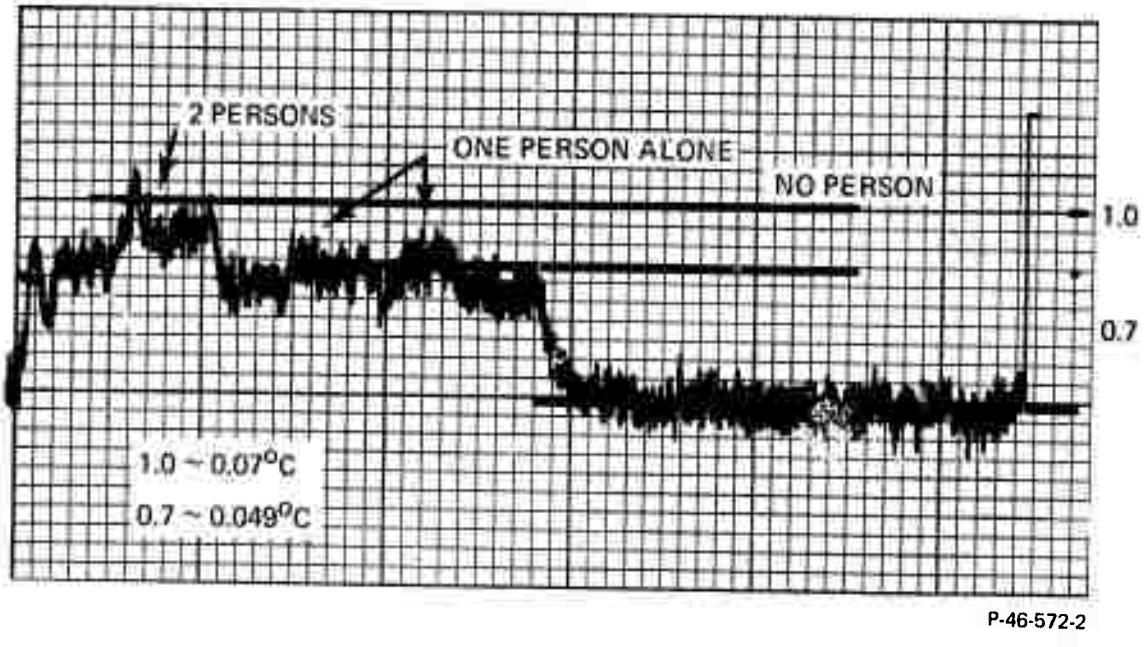

Figure 4-6 - Influence of Body Radiation on Rock Temperature Measurements

follows the trend of the air temperature, which is also lower near the floor.

4.1.2 Temperature Difference between Loose Rock and Solid Rock

On the site described in Section 4.1, the temperature was measured on loose gneiss about 2-1/2" thick[6]. Then the gneiss was broken off and the temperature of the freshly exposed rock was measured.

The temperature difference between the two measurements was on the order of 5×10^{-3}°C, with the freshly exposed rock having the higher temperature. This indicates that, even days after the air temperature in a mine has been changed, some loose rock can be detected with sufficiently sensitive temperature-measuring devices. The size of the signal is, however, not only a function of the time elapsed since the air temperature in the drift changed, but also a function of the thermal conductivity, the thermal capacitance, the volume of the loose rock, and the size of the contact area over which heat conduction occurs into the solid matrix rock. In the following, the complexity of the loose rock problem is discussed.

The model for the temperature behavior of a loose rock is as follows. Figure 4-8 shows a schematic of a loose rock with a total effective surface area F_1 exposed to air. It is separated from the matrix rock by a narrow air gap. The contact area, which in reality does consist of many area elements, is contracted into area F_2 for simplicity's sake. The rest is the solid matrix rock. The heat conduction through the air gap is also included in the effective F_2. The rock itself has an effective volume V. The heat transfer into the loose rock from the air occurs through a thin boundary layer of thickness (δ). The temperature of the loose rock is governed by the differential equation of conduction of heat in an isotropic solid:

$$\frac{1}{d} \times \frac{\partial T}{\partial t} = \nabla^2 T; \quad d = \frac{\kappa}{\rho C} = \text{diffusivity}$$

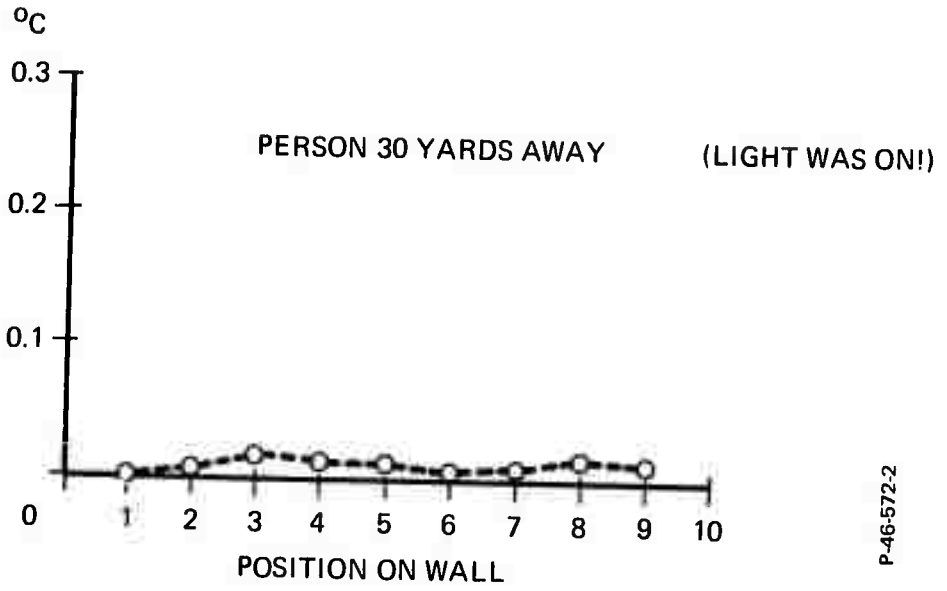

Figure 4-7 - Sweep Over Feldspar Intrusion (No Personnel Present)

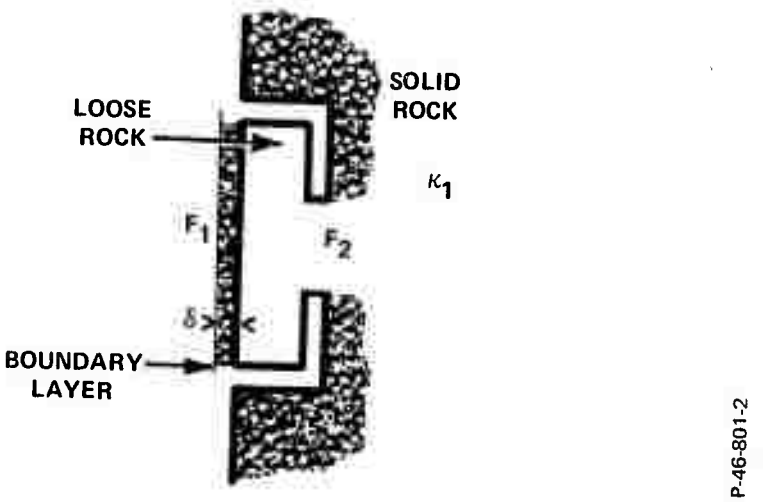

Figure 4-8 - Schematic of Loose Rock

The boundary conditions for which this equation must be solved are given by

$$\frac{dQ}{dt} = F_1\, k(T_{air} - T_{rock}) = F_1\, \kappa_1 \text{ grad } T_{rock}$$

where

$\frac{dQ}{dt}$ = total heat flow into rock per second.

k = heat transfer coefficient

κ_1 = thermal conductivity of rock near the surface F_1

T_{air} = air temperature

T_{rock} = temperature of air-exposed surface of loose rock.

The heat transfer coefficient depends on the air speed in the tunnel, the humidity of the rock, and the roughness of the rock surface, all of which can vary[7]. Furthermore, κ_1 grad T = κ_2 grad T in the contact region, where κ_2 is the effective conductivity due to the restricted area F_2.

It is obvious that a theoretical determination of the temperature of a loose rock as a function of time is not possible, even if the changes of air temperature are known, since k, κ_1, κ_2, F_1, and the volume are not known.

An interesting special case of loose rock was found in the Republic Steel Mine in Mineville, N. Y. In the chamber (a drift closed off with bulkheads) in which the Army performed their heat dissipation experiments, we found an equal distribution of surface temperature on the rock. There was no detectable temperature change. On close inspection, we found that the whole surface was covered with a spalled-off layer between 1/8- and 1/4-inch thick which apparently was at an equilibrium temperature all over the walls. Loose rock of larger dimension could lie beneath this thin layer without creating a temperature signal on the surface. The conclusion from this is that the absence of a temperature change on the walls or on the roof of a

drift does not necessarily mean that there is no loose rock. On the other hand, a change in apparent temperature does not necessarily mean that there is loose rock, since such a change can be caused by changes in emissivity, reflectivity, or possible moisture.

4.2 TEMPERATURE MAPPING FOR AN UNVENTILATED DRIFT

The objective of these measurements was to study the variation of temperatures over long distances in the mine to see if a basic temperature profile, representing the heat flow from the interior of the earth, could be detected. In Figure 4-9, the apparent temperature distribution along the drift 3A is plotted at ten-foot intervals. No special effort was made to avoid loose rock. The drift was excavated by blasting and shows the usual surface roughness. Many cracks of unknown depth were visible. The drift is not ventilated but opens into the main tunnel in which a constant air flow is maintained. The lithology is metamorphic gneiss. The altitude above sea level is 7800 feet and there is no slope.

During our measurements, we found places at which temperature differences of many hundredths of a degree occurred due simply to a difference in moisture on the rock. The moisture was deposited by the air exhaust of a drill a long time before and could only be water or oil absorbed by the rock. This moisture was only recognizable by the somewhat darker colors of the rock. The general trend of the temperature in drift 3A was an increase of temperature toward the middle of the drift and then a decrease toward the closed end. The change of the rock temperature over the drift length was almost two orders of magnitude higher than a temperature change caused by the bending of isotherms due to differences in lithology. The large changes observed are probably due to both air exchange with the main tunnel and, perhaps to some extent, the topography of the mountain in which the mine is located.

The measurements do show that very large temperature changes result from causes other than intrusions or inclusions, since no

intrusions exist in the mine that are large enough to account for the magnitude of the temperature change.

Drift B1 was also mapped and the results are given in Figure 4-10. In this case, an attempt was made to measure temperatures only on solid rocks having no detectable moisture. There is less fluctuation than in the first case, but still more than 0.01°C. The general trend from the closed end of the drift toward the main tunnel shows increasing temperature up to the location of a raise. Here work had been performed several hours before the measurements and fresh air had been blown into the raise. Therefore, the sudden drop of the rock temperature in the vicinity of the raise is probably due to the cold ventilation air from the main tunnel. The conclusion drawn from these measurements is again that the surface rock temperature in drifts is very much determined by the ventilation conditions in such drifts.

During the mappings, we had hoped that a trend in temperature distribution could be picked up which was definitely not attributable to the air temperature. This attempt, however, was not successful.

4.3 DETERMINATION OF INFLUENCE OF BLASTING ON ROCK TEMPERATURE MEASUREMENTS

An experiment was conducted to determine the influence which blasting has on the temperature of freshly exposed rock. At the closed end of drift B1, a site was chosen to check the temperature signature left on rock freshly exposed by blasting. Three holes spaced one foot apart were drilled into a protruding part of the wall in order to clean off an area of approximately 3' x 3' (see Figure 4-11). Only one stick of dynamite was used in each hole in order to keep the energy dissipated to a minimum. Figure 4-12 shows the source area after blasting. After about 20 minutes of ventilating with compressed air, the area was sufficiently dust-free to permit measurements with the radiometer. The freshly exposed rock between the shot holes increased as much as 0.09°C with respect to the old rock surfaces, with variations between the shot holes of 0.06°C. The locations at which the shot holes ended in the

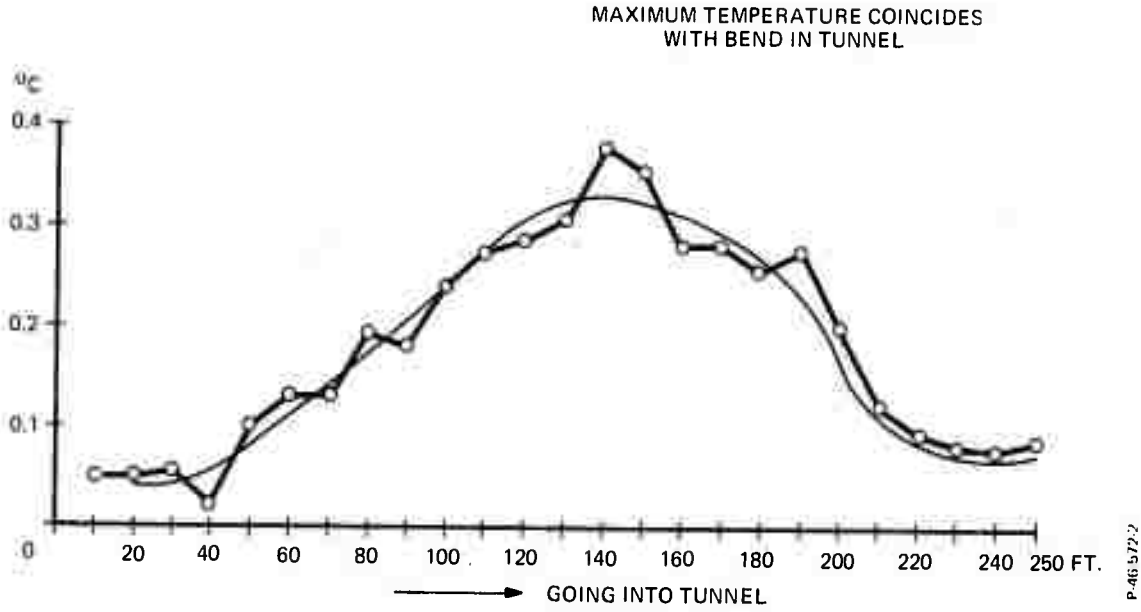

Figure 4-9 - Apparent Temperature Distribution Along Drift 3A

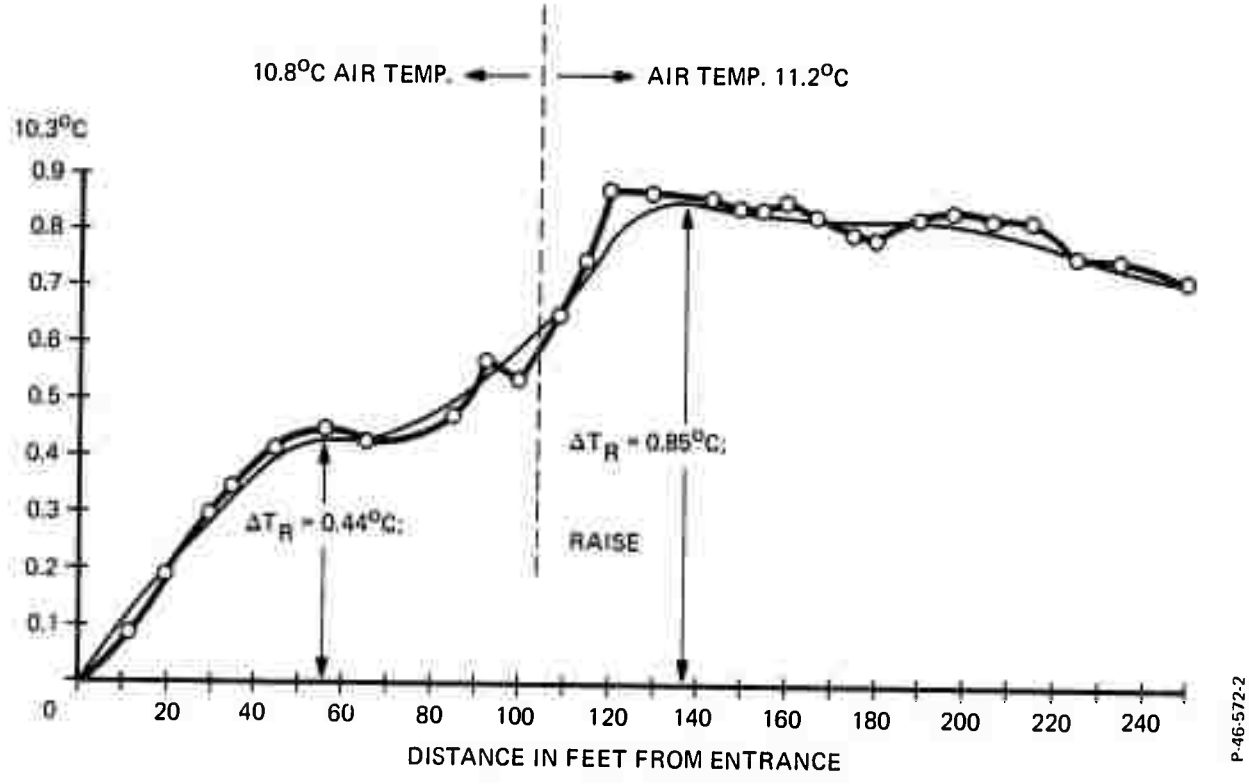

Figure 4-10 - Apparent Temperature Distribution Along Drift B1

Figure 4-11 - Rock Appearance Prior to Blasting

Figure 4-12 - Rock Exposed by Blasting

Reproduced from best available copy.

rock could be clearly identified as hot spots. After 17 hours, the temperature of the blast area was still 0.03°C higher than that of the undisturbed rocks, with the shot holes clearly the warmest spots. The results of this experiment indicate that thermal energy generated by blasting (and probably by excavation machinery) would be sufficient in itself to mask any change in temperature due to geological changes.

4.4 TEMPERATURE MAPPING ACROSS LARGE INTRUSION AT END OF DRIFT B1

This experiment was conducted because the intrusion of feldspar occurred at the end of an unventilated drift, excluding the influence of air temperature changes. Figure 4-13 schematically shows the closed end of drift B1 where the dark end face consists of mica shist. A photograph of this area can be found in Figure 4-14. A feldspar intrusion crosses a few feet ahead of the end of the drift and ahead of the feldspar, gneiss occurs. When the intrusion was scanned, a definite temperature minimum was detected that was lower than the temperatures of the mica shist and gneiss. The magnitude of this temperature change is similar to that detected on feldspar as compared to geniss (Section 4.1.1).

The magnitude of the temperature change in both cases would suggest that the feldspar and the gneiss were in equilibrium with the air temperature; otherwise the much larger pegmatite intrusion in the present case should have given a larger signal. Therefore, the "effective temperature" difference between the gneiss and the pegmatite is likely to be due to a difference in emissivity.

4.5 TEMPERATURE MAPPING OF A BORED SLOPED TUBE PENETRATING A MAGNETIC ORE BODY

The experimental site at the Republic Steel Mine chosen for the following measurements was an 8-foot diameter bored tube descending at 30 degrees, with a total length of 800 feet. The elevation difference between the entrance and the end of the tube is 400 feet.

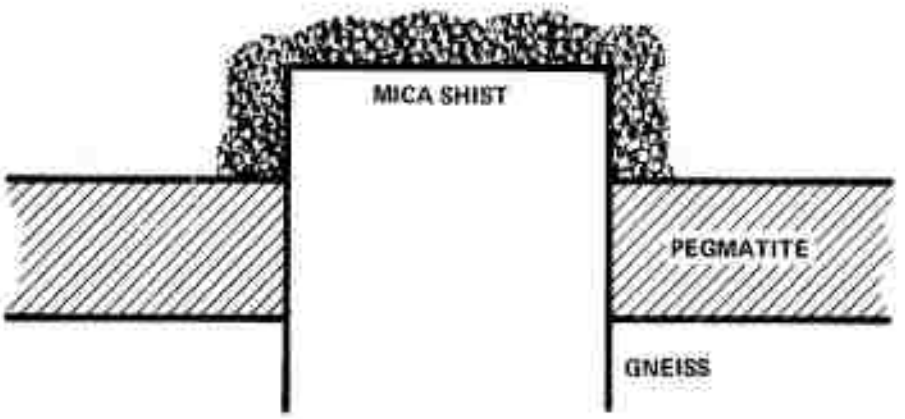

Figure 4-13 - Diagram of Closed End of Drift B1

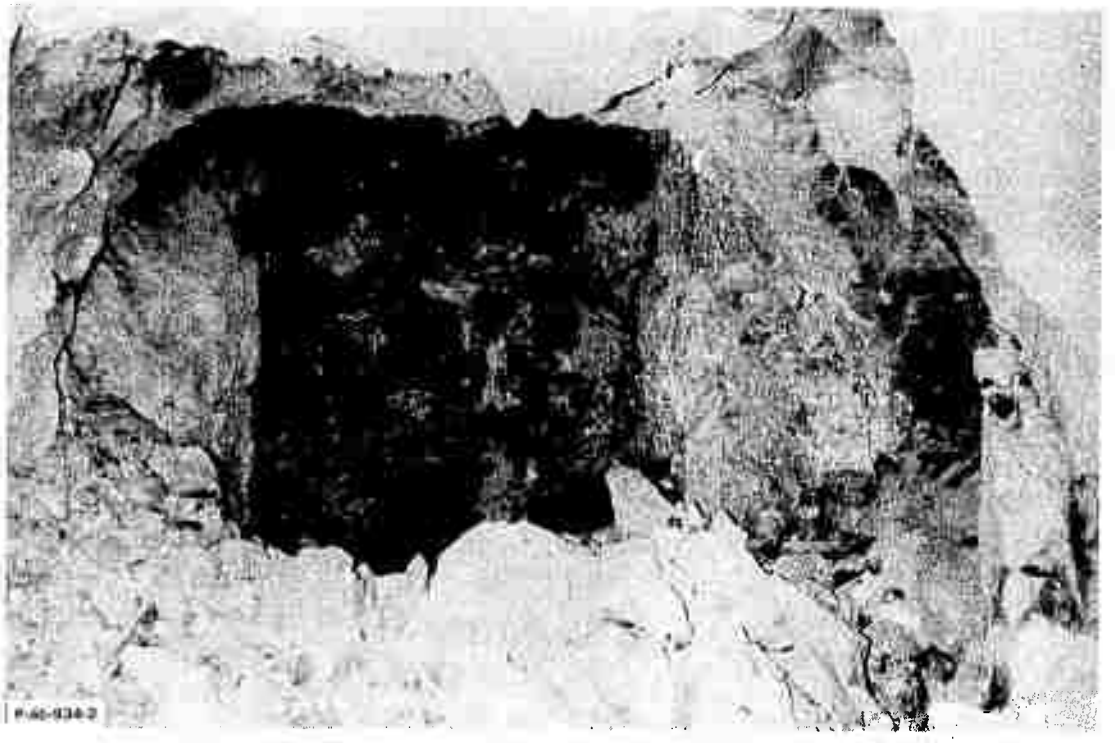

Figure 4-14 - Bored Tube at Republic Steel Mine

Figure 4-2 shows the general lithology with respect to this tube. The first 220 feet penetrates a rather large deposit of magnetite, which then gradually tapers away from the tunnel and is replaced by gneiss. The transition from magnetite to gneiss on the tube surface is rather sudden, so that the radiometer sees gneiss alone, although the magnetite is only inches below the surface. During these measurements, the air temperature was also determined using a precision thermometer. The latter values are plotted along with the measured wall temperatures in Figure 4-15. In general, both the air and wall temperature increase with depth, and the average wall temperature gradient is $\approx 1.4 \times 10^{-2}$°C/m, which is of the expected magnitude. Figure 4-15 shows that a very rapid increase of wall temperature occurs over the first 80 feet of the tube,

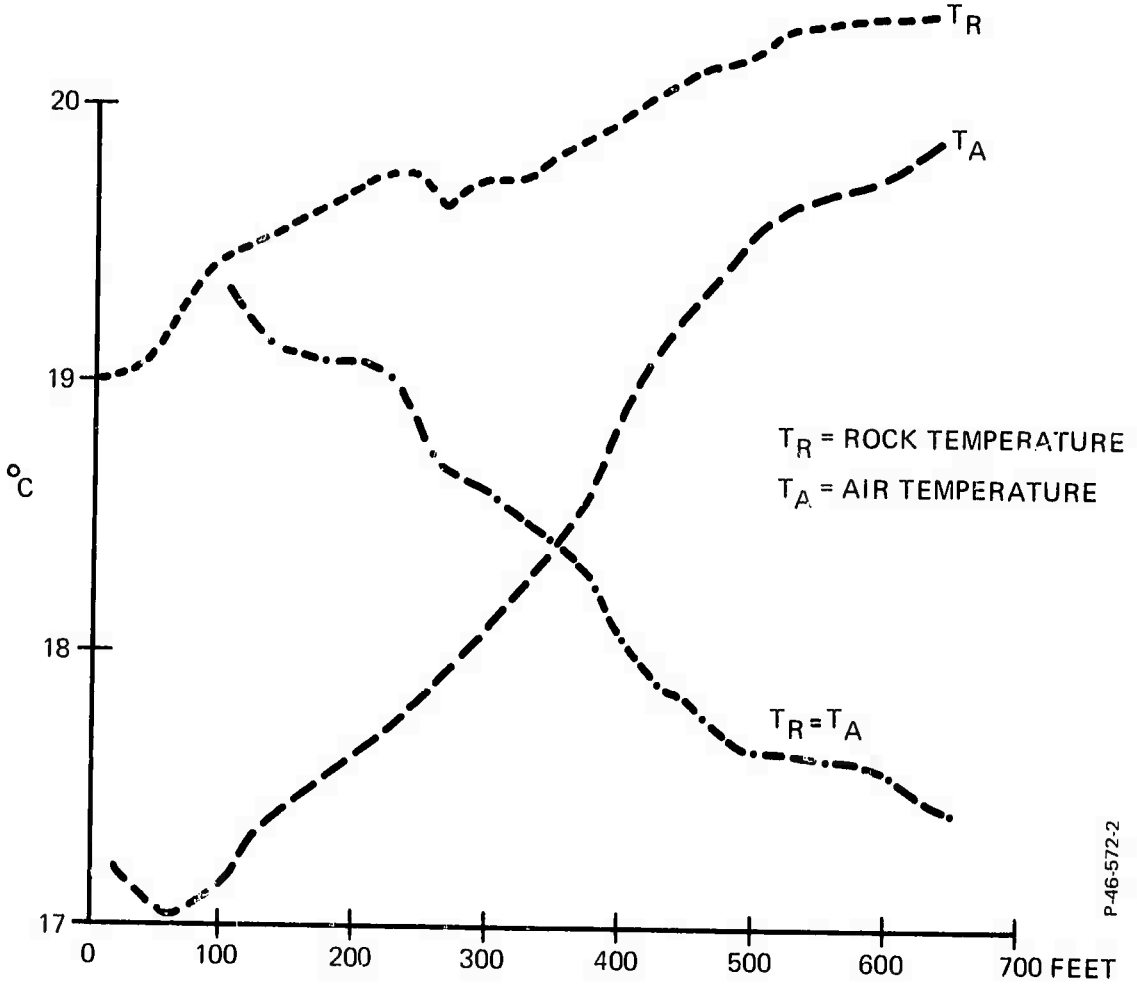

Figure 4-15 - Plot of Air Temperature and Rock Temperature for Bored Tube

probably due to the air currents from the main tunnel. From 80 feet up to 220 feet, the wall temperature follows a very smooth curve. It then levels off until 240 feet where it drops off sharply by 0.2°C and then again rises to a new plateau at 290 feet. From 320 feet on, the temperature curve is rather smooth except for a dip at about 480 feet. The curve finally flatens out at 640 feet. The last 160 feet could not be mapped because of debris and water at the end of the tube. The zones of special interest are the region between 220 feet and 300 feet and the region at 480 feet.

According to information obtained from the Republic Mine administration, the ore body is close to the tube walls at the region from 220 feet to 300 feet and apparently is slightly further away around the 480-foot area. This information then indicates that the detected signal is indeed due to wall temperature and not to changes in emissivity. Since the thermal conductivity of magnetite is almost twice that of gneiss, one would expect magnetite to show a higher temperature than gneiss. Oxidation of magnetite to hematite does not seem to be the cause for the higher temperature, since hematite has a characteristic red color which would be observed if this material were present. Thus, it seems that the mapping of temperatures in deep mines may be useful for locating ore bodies. Theoretical findings also support this conclusion.

In all these measurements, it has to be borne in mind, however, that the surface temperature of the rock is not the same as the temperature would be in undisturbed solid rock, since the surface exchanges heat with the air in the tube. In a case like the present one, where there is no forced air flow, one should obtain a more accurate temperature measurement by determining the energy transported in the air.

Whenever a temperature difference exists between the air and the tunnel walls, heat has to be transferred from the warmer to the colder medium. Since the tunnel walls are, in all locations, warmer than the air, the heat flow has to be from the rock into the air:

$$\frac{dQ}{dt} = k\ (T_{rock} - T_{air})$$

$$\frac{dQ}{dt} = -\kappa \frac{dT}{dx}$$

In the first equation, the heat flow from the rock into the air is given as a function of the difference between the rock and the air temperature and the heat transfer constant. In the second equation, the heat flow from the rock is given as a function of the temperature gradient in the rock very close to the surface and the thermal conductivity of the rock.

By measuring the air flow and the air temperature along the tunnel, one could determine the heat contribution from the unit length of the tunnel, which is equivalent with an averaged $\frac{dQ}{dt}$. Knowing this yields $\frac{dT}{dx}$ under the surface and thus enables one to correct the rock surface temperature for its deviation from the internal rock temperature.

Theoretically this is possible, but practically this correction would require rather complex equipment to measure the heat transport in the air.

4.6 SUMMARY OF EXPERIMENTAL RESULTS

The temperature measurements show conclusively that very large areas of geological change will create a temperature change large enough to be detected by a radiometer. However, IR-radiating sources (due to the variation in reflectivity of rocks of different color and composition), changes in emissivity, changes in air temperature, and barely visible amounts of dampness on rocks can cause temperature changes many times larger than the signal to be observed. Even if one were to go through the time-consuming task of determining the emissivity of the rocks at each point of readiometer measurements, one would still have to deal with the air temperature and the dampness. Both of these factors are difficult to control in a mining environment.

SECTION 5
CONCLUSIONS

The outcome of this project is the following. The theoretical analysis indicates quite clearly that the determination of the size and the location of an area of change in lithology is not possible. The analysis did indicate the possibility of distinguishing between changes of lithology, water-bearing sources, and geothermal sources as long as the temperature changes which occur are in the range of a few hundredths of a degree centigrade. Once the temperature change exceeds a few hundredths of a degree, one can assume a geothermal source. However, safety would require that precautions be taken for the smallest detectable change. The excavating process would have to be interrupted and probing holes would have to be drilled.

The procedure documented in this report in only applicable for cases where the temperature of the walls of a drift or tunnel are not obscured by temperature changes caused by air currents, water vapor, or heat from either explosives or equipment. In the experimental part of the project, we found that reflected radiation from human bodies was sufficient to simulate signals many times the size of those caused by rock temperature changes. Even on drift walls which had been in equilibrium with the air for a long time, temperature fluctuations were observed which were of the size of, or larger than, the signals of interest. Some of these fluctuations could be correlated with dampness of the rocks and dust.

Only in the case of very large inclusions (many tens of meters) could a signal change be observed and attributed to the presence of an ore body. It is for this case that the thermal monitoring method is potentially useful. In a mine with many levels and many drifts on the same level, temperature mapping with no ventilation in the drifts might

yield information concerning the presence of undetected ore bodies. This possibility would have to be explored experimentally.

Thus, we conclude that thermal monitoring as a method for predicting hazards in rapid excavation is not reliable.

SECTION 6

REFERENCES

1. Y. C. Yaeger, "Thermal Effects of Intrusions," Reviews of Geophysics 2, 3, (August 1964).
2. H. S. Carslaw and Y. C. Yaeger, Conduction of Heat, Oxford Press.
3. Henry L. Hackforth, Infrared Radiation, McGraw-Hill, New York, 1960.
4. P. P. Feofilov, The Physical Basis of Polarized Emission, Consultants Bureau, New York, 1961.
5. W. F. Quinn, H. W. C. Aamot, M. Greenberg, "Analysis and Test of a Rock-Steam Condenser Heat Sink Concept," ASME Publication-HTD, Volume 4.
6. R. H. Merrill, R. M. Stateham, "Loose Rock Can Be Detected by Infrared Devices," Mining Engineering (November 1970).
7. M. Jacob, Heat Transfer, John Wiley & Sons, Inc., N. Y., 1958.